EUROPEAN ORGANIZATION FOR NUCLEAR RESEARCH (CERN)

CERN-EP-2026-066
2026/09/09

CMS-HIN-24-021

Measurement of the top quark pair production cross section in PbPb collisions at $\sqrt{s_{\mathrm{NN}}} = 5.36\,\mathrm{TeV}$

The CMS Collaboration*

arXiv:2604.27091v2 [nucl-ex] 5 Sep 2026

Abstract

The inclusive cross section for top quark pair ($\mathrm{t\bar{t}}$) production in lead-lead (PbPb) collisions is reported for the first time at a center-of-mass energy per nucleon pair of 5.36 TeV. The analysis uses data corresponding to an integrated luminosity of $1.58\,\mathrm{nb}^{-1}$ collected by the CMS experiment at the CERN LHC in 2023. The $\mathrm{t\bar{t}}$ production cross section, $\sigma_{\mathrm{t\bar{t}}} = 3.42^{+0.54}_{-0.51}\,(\mathrm{stat})^{+0.50}_{-0.43}\,(\mathrm{syst})\,\mu\mathrm{b}$, is measured in dilepton final states using a fit to a multivariate discriminator that combines the decay electron and muon kinematic properties with the multiplicity of bottom quark jets. The result is consistent with perturbative quantum chromodynamics calculations at next-to-next-to-leading order (NNLO) accuracy employing several nuclear parton distribution functions. In addition, the Drell–Yan production cross section (σ_{DY}) for dilepton masses above 10 GeV and the ratio of $\mathrm{t\bar{t}}$ to DY cross sections ($R_{\mathrm{t\bar{t}/DY}}$) are found to be compatible with the NNLO predictions. The observables $\sigma_{\mathrm{t\bar{t}}}$, σ_{DY}, and $R_{\mathrm{t\bar{t}/DY}}$ are measured separately for central and semicentral PbPb collisions to investigate for the first time the dependence of top quark production on the collision impact parameter.

Published in the Journal of High Energy Physics as doi:10.1007/JHEP08(2026)054.

© 2026 CERN for the benefit of the CMS Collaboration. CC-BY-4.0 license

*See Appendix A for the list of collaboration members

1 Introduction

Extensive studies of the cross section and properties of top quark-antiquark pairs ($\mathrm{t\bar{t}}$) produced in proton-proton (pp) collisions at the CERN LHC [1, 2] have improved our knowledge of key fundamental parameters of the standard model, such as the top quark mass (m_{t}), the strong coupling constant (α_{S}), and the Yukawa coupling of the top quark to the Higgs boson, through comparisons of the data with high-accuracy perturbative quantum chromodynamics (pQCD) predictions. These measurements have also contributed to determining the parton distribution functions (PDFs) of the proton with reduced uncertainties. In heavy ion collisions, the production of top quarks has long been proposed as a powerful probe of the nuclear gluon density at high virtualities [3], as encoded in nuclear PDFs (nPDFs). It has also been proposed as a useful means to study final-state effects on top quark decay products as they traverse the produced quark-gluon plasma (QGP), where they may experience parton energy loss in the medium ("jet quenching") [3, 4].

Because the top quark decays almost exclusively as $\mathrm{t} \to \mathrm{Wb}$ [5], a $\mathrm{t\bar{t}}$ event contains two b jets and the decay products of the two W bosons. Experimentally, $\mathrm{t\bar{t}}$ events are classified according to the W boson decay modes. About 46% of $\mathrm{t\bar{t}}$ events are fully hadronic, but these are difficult to isolate from quantum chromodynamics (QCD) multijet backgrounds, which have much larger cross sections. Events in which only one W boson decays leptonically account for roughly 45% of the total; however, their final states contain multiple jets and are subject to systematic uncertainties from jet energy calibration, quark flavor tagging, and combinatorial ambiguity. The dilepton decay mode, $\mathrm{t\bar{t}} \to (\mathrm{W^+b})(\mathrm{W^-\bar{b}}) \to (\ell^+\nu_\ell \mathrm{b})(\ell^-\bar{\nu}_\ell \mathrm{\bar{b}})$, provides the cleanest experimental signature, even though its branching fraction is about 4% when restricting ℓ to electrons and muons. This channel yields a pure (>95%) sample with relatively loose lepton selection requirements. In pp collisions, the single lepton [6] and dilepton [7] channels provide the most precise measurements of the $\mathrm{t\bar{t}}$ production cross section. Among all channels, the $\mathrm{e^{\mp}}\mu^{\pm}$ final state typically provides the best sensitivity. Owing to its higher purity and nearly twice the event yields of the same flavor ($\mathrm{e^+e^-}$ or $\mu^+\mu^-$) channels, the $\mathrm{e^{\mp}}\mu^{\pm}$ final state is used to measure the $\mathrm{t\bar{t}}$ production cross section with lower uncertainties. In the heavy ion environment, the presence of a very large hadronic background makes it more challenging to measure the lepton + jets decay final states. For these reasons, the dilepton final state, including events with tau leptons that decay into an electron or a muon, is commonly adopted to measure the $\mathrm{t\bar{t}}$ production cross sections.

The production of top quark pairs has been measured in proton-lead collisions at a nucleon-nucleon (NN) center-of-mass energy of $\sqrt{s_{\mathrm{NN}}} = 8.16\,\mathrm{TeV}$ [8, 9] and in lead-lead (PbPb) collisions at $\sqrt{s_{\mathrm{NN}}} = 5.02\,\mathrm{TeV}$ [10, 11]. The early PbPb collision measurements used data corresponding to 1.7–1.9 $\mathrm{nb^{-1}}$ of integrated luminosity. They have proved useful to establish the baseline observables and selection criteria in the dilepton channel, confirming the feasibility of top quark measurements in events with very large particle multiplicities. However, the ability of these studies to constrain nPDFs or the properties of QGP is limited by the poor statistical precision of the datasets analyzed.

This paper reports the first measurement of the inclusive production cross section of $\mathrm{PbPb} \to \mathrm{t\bar{t}}$ at $\sqrt{s_{\mathrm{NN}}} = 5.36\,\mathrm{TeV}$, utilizing data corresponding to an integrated luminosity of $1.58\,\mathrm{nb^{-1}}$ collected in 2023. The analysis uses advanced algorithms to select leptons and identify jets stemming from the fragmentation and hadronization of b quarks (b jets). These improved techniques combine new variables used to characterize the isolation and prompt production of leptons from $\mathrm{t\bar{t}}$ events, and make use of new discriminants based on machine learning to identify the decay leptons, as well as the b jets. By incorporating these novel algorithms and

performing a combined fit to a multivariate $\mathrm{t\bar{t}}$ discriminant across several event categories, the analysis improves upon previous results, reducing the uncertainty in the $\sigma(\mathrm{PbPb} \to \mathrm{t\bar{t}})$ cross section and enabling the first observation of this process in heavy ion collisions by the CMS experiment.

The paper is structured as follows. The experimental apparatus is presented in Section 2, and the simulation and event selections are described in Sections 3 and 4, respectively. The methods used to control the backgrounds and to extract the signal are described in Sections 5 and 6, respectively. The results are presented in Section 7, and summarized in Section 8. Tabulated results of the analysis can be found in HEPData [12].

2 The CMS detector

The CMS apparatus [13, 14] is a multipurpose, nearly hermetic detector, designed to trigger on [15–17] and identify electrons, muons, photons, and (charged and neutral) hadrons [18–20]. Its central feature is a superconducting solenoid of 6 m internal diameter, providing a magnetic field of 3.8 T. Within the solenoid volume are a silicon pixel and strip tracker, a lead tungstate crystal electromagnetic calorimeter (ECAL), and a brass and scintillator hadron calorimeter (HCAL), each composed of a barrel and two endcap sections. Muons are reconstructed using gas-ionization detectors embedded in the steel flux-return yoke outside the solenoid. Forward calorimeters extend the pseudorapidity (η) coverage provided by the barrel and endcap detectors. Two forward hadron (HF) calorimeters use steel as an absorber and quartz fibers as the sensitive material. They are located 11.2 m from the interaction region, one on each end, and together they provide coverage in the range $3.0 < |\eta| < 5.2$. They also serve as luminosity monitors. In addition, two zero-degree calorimeters (ZDCs), made of quartz fibers and plates embedded in tungsten absorbers, are used to detect neutrons (n) from nuclear breakup events in the range $|\eta| > 8.3$ [21]. More detailed descriptions of the CMS detector, together with a definition of the coordinate system used and the relevant kinematic variables, can be found in Refs. [13, 14].

Events of interest are selected using a two-tiered trigger system. The first level, composed of custom hardware processors, uses information from the calorimeters and muon detectors to select events at a rate of up to 70 kHz within a fixed latency of 4 μs [15]. The second level, known as the high-level trigger (HLT), consists of a farm of processors running a version of the full event reconstruction software optimized for fast processing, and reduces the event rate down to 50 kHz before data storage [16, 17]. The quoted values have been optimized for PbPb collisions.

A particle-flow (PF) algorithm [22] aims to reconstruct and identify each individual particle in an event, with an optimized combination of information from the various elements of the CMS detector. The energy of photons is obtained from the ECAL measurement. The energy of an electron is determined from a combination of the electron momentum at the primary interaction vertex as determined by the tracker, the energy of the corresponding ECAL cluster, and the energy sum of all bremsstrahlung photons spatially compatible with originating from the electron track. The energy of a muon is obtained from the curvature of the corresponding track. The energy of a charged hadron is determined from a combination of the momentum measured in the tracker and the matching ECAL and HCAL energy deposits, corrected for the response function of the calorimeters to hadronic showers. Finally, the energy of neutral hadrons is obtained from the corresponding corrected ECAL and HCAL energies.

3 Monte Carlo simulations

Monte Carlo (MC) simulations are used to estimate the signal acceptance and efficiency, as well as to validate the background estimation methods. The simulations are performed using matrix element (ME) generators based on pQCD calculations at next-to-leading order (NLO) accuracy, emulating a mixture of pp, pn, and nn interactions in proportions corresponding to their relative abundances in lead nuclei (mass number $A = 208$). The ME generators employ the EPPS21_nlo nPDFs [23], which use the CT18ANLO PDF [24] as the proton parton density baseline. The generated events are then interfaced with the PYTHIA 8.306 [25] parton shower (with the CP5 tune [26]) and are embedded in inelastic PbPb events simulated with the HYDJET [27] MC generator. The HYDJET model reproduces the effects of the underlying event (UE) measured in PbPb data. In doing so it does not alter the hard-scattering process simulated at the ME level, nor the decay products of the generated particles. To account for possible medium effects affecting the simulated signal and background final states, methods based on data are employed and described in more detail at the end of Section 4. The PbPb collision "centrality" (i.e., the degree of overlap of the two Pb ions) is determined from the sum of the transverse energy ($\sum E_T$, where $E_T = E \cosh \eta$), deposited in both HF calorimeters and corrected with an event-by-event weighting procedure based on the average number of NN collisions in each centrality interval as obtained with a Glauber model [28]. After this weighting, residual differences between the centrality distribution measured in data and predicted in simulation are corrected for based on a control sample of $Z \to \mu^+\mu^-$ events. All the MC samples include a simulation of the full detector response implemented in GEANT4 [29] with realistic alignment and calibration, tuned to data.

The MC $t\bar{t}$ signal samples are generated at NLO accuracy with MADGRAPH5_aMC@NLO (v2.9.18) [30] and POWHEG v2 [31]. In the former case, the event generation includes up to two extra partons at the ME level, and the merging with the parton shower is performed via the FxFx procedure [32]. In the POWHEG case, only up to one real parton emission is generated, with the remainder produced by the parton shower. The cross sections of both simulated $t\bar{t}$ samples are scaled up to match the next-to-next-to-leading order (NNLO) pQCD predictions, including soft-gluon resummation at next-to-next-to-leading logarithmic (NNLL) accuracy, obtained with the TOP++ program [33]. In the calculation a top quark mass of $m_t = 172.5\,\text{GeV}$ is used, the nominal renormalization and factorization scales are set to $\mu_R = \mu_F = m_t$, and the QCD strong coupling is set to $\alpha_S(m_Z) = 0.118$. Uncertainties of $\pm 1.0\,\text{GeV}$ and ± 0.001 are assumed for the m_t and $\alpha_S(m_Z)$ values [5], respectively. The predicted NNLO + NNLL inclusive cross section is $\sigma_{th}(\text{PbPb} \to t\bar{t}) = 3.69^{+0.71}_{-0.48}\,\mu\text{b}$, where the uncertainty is the quadratic sum of theoretical scale, parametric (from m_t and α_S), and EPPS21_nlo nPDF uncertainties.

The characteristic signature of the $t\bar{t}$ events selected in this analysis is the presence of two leptons with large transverse momentum (p_T) originating from the W^+W^- decays. Consequently, any process that produces a similar dilepton final state can mimic the signal and constitutes a background to the measurement. The simulated background samples include Drell–Yan (DY, $Z/\gamma^* \to e^+e^-/\mu^+\mu^-/\tau^+\tau^-$), W + jets, single top quark production, diboson processes, and multijet events containing nonprompt leptons, mostly from heavy-quark hadron decays. The inclusive DY process $pp \to Z + X$, including up to two recoiling jets via the FxFx merging procedure, is simulated with MADGRAPH5_aMC@NLO separately in the low-mass (10–50 GeV) and high-mass (>50 GeV) regions, with predicted cross sections of 287 and 83 μb, respectively. The same generator is used for the W + jets sample, with a cross section of 899 μb . Single top quark production in association with a W boson or via the t channel is simulated with POWHEG [34], with corresponding cross sections of 0.272 and 1.27 μb. Diboson events, in particular WW, are

generated with POWHEG including all final states with at least one lepton. The WW contribution is normalized to a cross section of 0.613 μb, as predicted by POWHEG. Finally, multijet processes with at least one muon or electron are simulated with PYTHIA. The multijet samples are included in the training of the lepton isolation discriminators, but are not used to estimate any of the backgrounds.

4 Event selection

Candidate events are first selected based on whether they pass the minimum-bias or the single-muon HLT triggers. The minimum-bias trigger requires a coincident signal in both HF calorimeters and the presence of at least one neutron in one of the ZDCs, whereas the single-muon trigger requires a muon reconstructed at the HLT with $p_{\mathrm{T}} > 7\,\mathrm{GeV}$. The stability of these triggers is verified throughout the data-taking period, and their efficiency is extracted directly from the data. Offline, collision events are further required to have at least one interaction vertex reconstructed with two or more tracks within a distance of 25 cm from the nominal collision point along the beam axis and 2 cm in the transverse plane. In addition, at least two towers (arrays of channels) on each side of the HF calorimeter must have a total reconstructed energy larger than 4 GeV.

Events containing at least two charged leptons—where "lepton" (denoted by ℓ) refers exclusively to electrons and muons hereafter—are selected, with additional criteria applied to target dilepton decays of the two W bosons from $\mathrm{t\bar{t}}$ production. Lepton candidates must have $p_{\mathrm{T}} > 20\,\mathrm{GeV}$, originate promptly from the primary collision vertex, and be isolated from other particles in the event. Electrons are required to lie within the ECAL barrel or endcap fiducial regions ($|\eta| \in [0, 1.444] \cup [1.566, 2.5]$), and muons are selected within $|\eta| < 2.4$. Candidates passing these kinematic and fiducial selections are further considered in the analysis if they satisfy two distinct sets of identification and isolation criteria. Decoupling these two requirements enables the isolation variable to define control regions (CRs), which are used to estimate the nonprompt-lepton background and extrapolate it to the signal region.

Electron identification relies on a dedicated boosted decision tree (BDT) discriminant that combines several observables, including the shower shape and position of the ECAL cluster, its matching to the associated reconstructed track, and the energy deposits in the HCAL towers subtended by the ECAL cluster. The BDT is trained on QCD multijet and $\mathrm{t\bar{t}}$ simulations using XGBOOST [35] and optimized with a grid-search cross-validation procedure [36]. An electron candidate is considered to pass the identification requirement if the BDT discriminant exceeds a centrality-dependent threshold corresponding to a 95% efficiency and an expected misidentification rate below 4%. This procedure ensures a selection efficiency independent of the collision centrality. The contamination from misidentified electron candidates is significantly reduced with respect to the rectangular-based identification criteria used in our previous study [10]. Muon identification is based on a set of quality requirements applied to the global track fit, which combines information from the inner tracker and the muon system. The selection follows the standard "tight" criterion described in Ref. [19].

For the isolation criteria, a common procedure applicable to both electrons and muons has been further developed, making use of dedicated BDTs trained separately for each lepton type. These BDTs combine different isolation sums of PF candidate energies within cones of radius $R = \sqrt{(\Delta\eta)^2 + (\Delta\phi)^2} = 0.3$ around the lepton direction. These isolation sums are computed using the "soft killer" method [37] with thresholds estimated in binned ranges of detector pseudorapidity, namely $[-2.5, -2, -0.8, 0.8, 2, 2.5]$. This procedure effectively mitigates the

dependence of the isolation sums on the PbPb event activity and enables a robust multivariate discrimination, less reliant on the simulation model used. In addition, the isolation BDT makes use of the three-dimensional impact parameter significance of each lepton. This variable is largely uncorrelated with the isolation sums and provides good discrimination against leptons from heavy-quark hadron decays. As for the electron identification BDT case, the independence of the working point on centrality ensures that the isolation requirement has a constant efficiency of 90%.

In case more than two leptons pass the selections above, priority is given to muons over electrons. The efficiencies associated with the trigger, identification, and isolation selections are determined using the tag-and-probe method based on $Z \to \ell^+\ell^-$ events in data [18, 19]. To improve the identification of the signal, the selected events are further categorized as follows:

- "SF/DF" labels indicate whether the leptons have the same (e^+e^- or $\mu^+\mu^-$) or different ($e^\mp\mu^\pm$) flavors. For SF final states, it is required that the acoplanarity $A_\phi = 1 - |\Delta\phi(\ell^+\ell^-)|/\pi$ is larger than 0.01 to remove contributions from elastic two-photon production ($\gamma\gamma \to \ell^+\ell^-$) [38].
- "SS/OS" labels indicate whether the leptons have the same or opposite electric-charge signs.
- "on-Z/off-Z" labels indicate whether the invariant mass of the SF OS pair is $|m(\ell\ell) - 91\,\text{GeV}| < 15\,\text{GeV}$ or $|m(\ell\ell) - 91\,\text{GeV}| > 15\,\text{GeV}$. Events with SF OS dilepton invariant mass $m(\ell\ell) < 20\,\text{GeV}$ are excluded to remove background contributions from quarkonia decays and the low-mass DY process.

To improve the discrimination from the main backgrounds, three additional BDT classifiers are trained for the e^+e^-, $e^\mp\mu^\pm$, and $\mu^+\mu^-$ final states. The BDTs make use of the following lepton-based variables:

1. the p_T of the leading (i.e., highest p_T) and subleading leptons: $p_T(\ell_1)$, $p_T(\ell_2)$;
2. the asymmetry of the leptons' p_T: $[p_T(\ell_1) - p_T(\ell_2)]/[p_T(\ell_1) + p_T(\ell_2)]$;
3. the p_T and mass of the dilepton system: $p_T(\ell\ell)$, $m(\ell\ell)$;
4. the sphericity of the dilepton system: $p_T(\ell\ell)/[p_T(\ell_1) + p_T(\ell_2)]$;
5. the absolute pseudorapidity of the dilepton system: $|\eta(\ell\ell)|$;
6. the sum of the lepton pseudorapidities: $\sum|\eta_\ell|$; and
7. the acoplanarity A_ϕ of the dilepton system.

Among these, $p_T(\ell\ell)$ and $m(\ell\ell)$ are found to be the most discriminating variables for the SF channels, whereas $p_T(\ell_2)$, $\sum|\eta_\ell|$, and $p_T(\ell\ell)$ are the most relevant observables in the DF final state. The relative importance of all input features has been quantified using a SHAP ranking [39]. The corresponding distributions are shown in Figs. 1 and 2 for the same- and different-flavor channels, respectively. Overall, a good agreement between data and MC expectations is found within the statistical uncertainties, prior to the fit to data. The training of the classifier is performed using the $t\bar{t}$ (signal) and DY (background) simulations and the XGBOOST package. In the training we have employed a cross-validation procedure and the OPTUNA algorithm [40] for the optimization of the hyperparameters. In order to improve the sensitivity of the analysis to the $t\bar{t}$ signal, the BDT discriminator has been evaluated separately for events with zero, one, or at least two b jets.

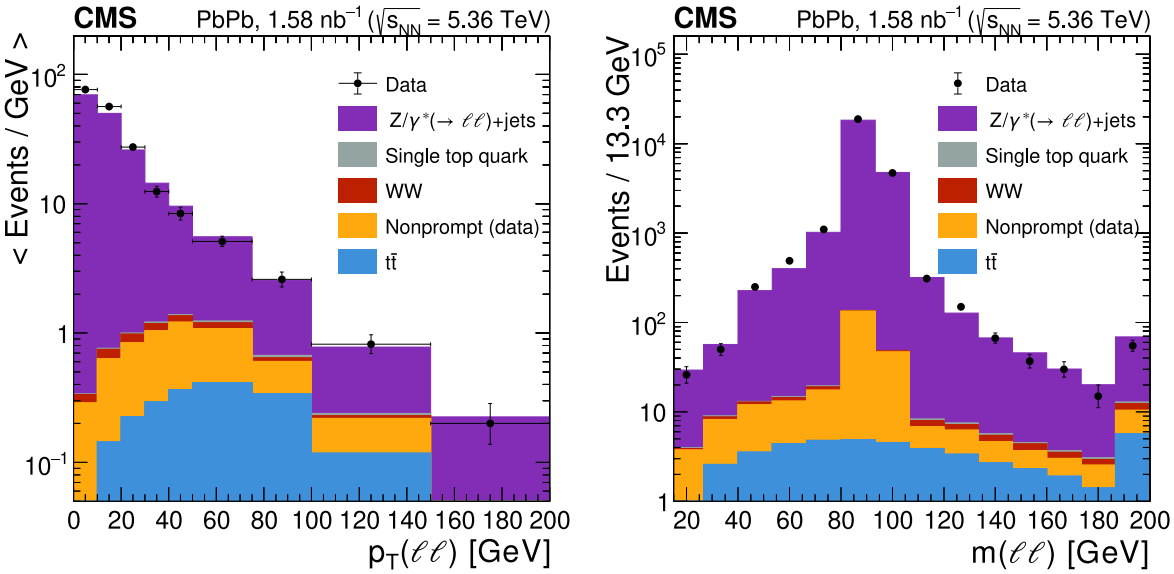


Figure 1: Distributions of dilepton $p_T(\ell\ell)$ (left) and invariant mass $m(\ell\ell)$ (right) variables in the same-flavor ($\ell\ell$) channels. The $m(\ell\ell)$ distribution is shown before applying the veto of the Z boson resonant region. The data (black markers with error bars representing statistical uncertainties) are overlaid on top of the stacked contributions from the expected $t\bar{t}$ (blue), nonprompt (light orange), WW (red), single top quark (gray), and DY (violet) processes. The last bin includes the overflow entries. In the left panel, the event counts are divided by the variable bin width.

For each event, hadronic jets are clustered from the PF candidates using the anti-k_T algorithm [41, 42] with a distance parameter of 0.3. Jet energy corrections and b quark identification are performed with a dedicated multivariate algorithm called "unified particle transformer" (UPART) [43], explicitly trained for heavy ion collisions. A detailed description of this algorithm for heavy-flavor quark identification can be found in Refs. [44, 45]. Jets with $p_T > 30$ GeV, $|\eta| < 2.1$, and separated from the lepton by a distance $\Delta R(\ell, j) > 0.4$ are accepted in the analysis. Three working points are defined for the identification of b jets: loose, intermediate, and tight; corresponding to b quark tagging efficiencies of 90, 80, and 70%, respectively. The intermediate working point is chosen as the default one in the analysis. These working points are parameterized such that the efficiency in simulation is constant as a function of collision centrality. The use of UPART reduces the misidentification rate by more than an order of magnitude relative to the b jet identification algorithm employed during Run 2 [10]. This improvement stems from the explicit exploitation of the jet PF constituent information within a transformer architecture, in contrast to the Run-2 approach that relied primarily on higher-level variables. In addition, the resulting jet energy scale correction becomes largely independent of the collision centrality (ignoring potential "jet quenching" effects) and remains robust with respect to the hadronization model, while retaining a residual dependence on the jet flavor.

The residual jet energy scale factor has been studied using Z boson events with $p_T(Z) > 30$ GeV and a jet recoiling in the transverse plane, $|\Delta\phi(Z, \text{jet})| > 2\pi/3$. In this control region, the simulation indicates that a significant fraction of the jets originates from genuine recoil contributions, with a smaller component arising from UE jets. Figure 3 shows the results of fits to the $x_j = p_T(\text{jet})/p_T(Z)$ variable for such Z + jet events in the 0–10% (left) and 10–90% (right) PbPb centrality bins. The distribution of recoil jets is modeled using a Crystal Ball function [46] (black dashed curves), with parameters determined directly from the fit. The UE contribution (gray

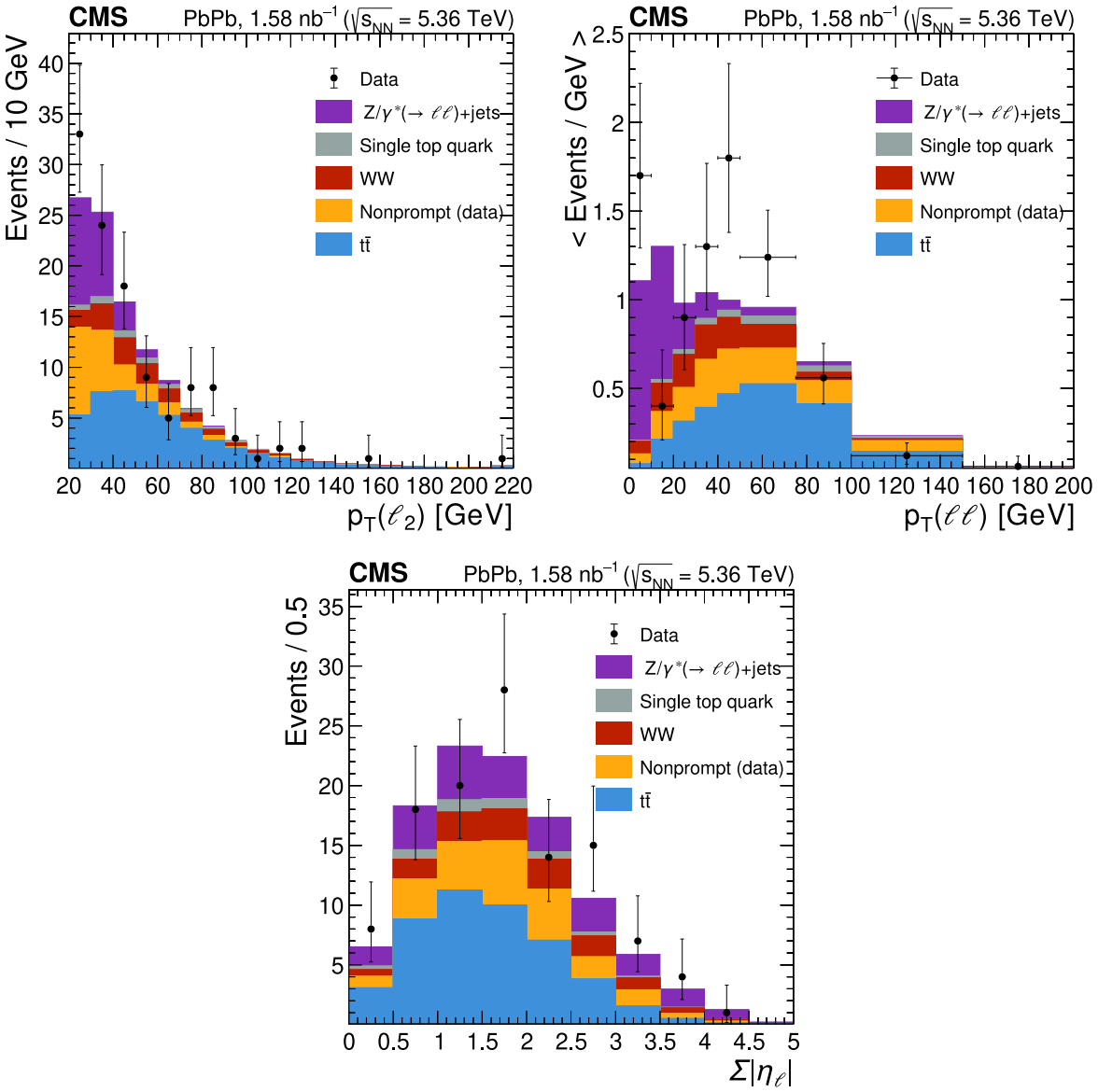


Figure 2: Distributions of $p_T(\ell_2)$ (upper left), $p_T(\ell\ell)$ (upper right), and $\sum|\eta_\ell|$ (lower) variables in the different-flavor ($e^{\mp}\mu^{\pm}$) channel. The data (black markers with error bars representing statistical uncertainties) are overlaid on top of the stacked contributions from the expected $t\bar{t}$ (blue), nonprompt (light orange), WW (red), single top quark (gray), and DY (violet) processes. The last bin includes the overflow entries.

histograms) dominates in events in which the jet is found in the near-side, or "toward," region relative to the Z boson direction, $|\Delta\phi(\mathrm{Z,jet})| < \pi/3$. The corresponding $x_\mathrm{j} = p_\mathrm{T}(\mathrm{jet})/p_\mathrm{T}(\mathrm{Z})$ distribution is modeled with the sum of a Crystal Ball and an exponential function. In the fit of $x_\mathrm{j} = p_\mathrm{T}(\mathrm{jet})/p_\mathrm{T}(\mathrm{Z})$, the UE-jets probability density function is fixed and its normalization floats with a Gaussian constraint. The combined recoil + UE-jets model (blue solid curves) reproduces well the data.

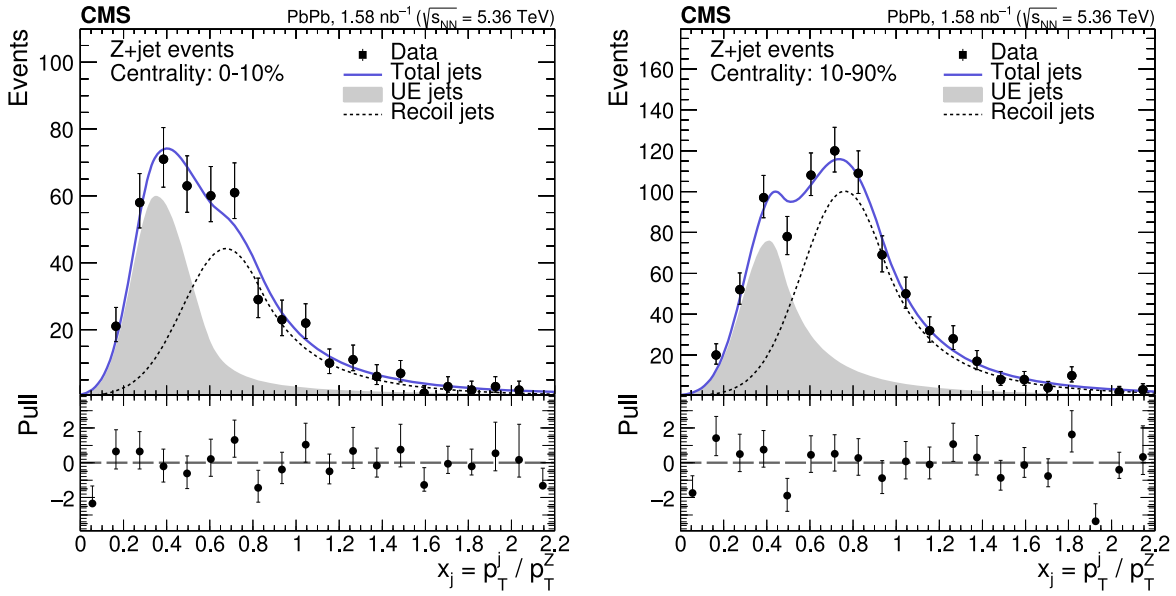


Figure 3: Distribution of the $x_\mathrm{j} = p_\mathrm{T}(\mathrm{jet})/p_\mathrm{T}(\mathrm{Z})$ ratio in Z + jet events in the 0–10% (left) and 10–90% (right) PbPb centralities. The data (solid dots with error bars) are compared with the contributions from UE jets (gray histograms) and true recoil jets (black dashed curves) stacked. The blue curves show the sum of UE and recoil jet contributions.

Among all the parameters of the fit, the mean of the Crystal-Ball function is used as a measurement of the average jet energy response, $\langle x_\mathrm{j} \rangle$. The $\langle x_\mathrm{j} \rangle$ profile provides a measure of the residual jet energy response dependence on the collision centrality (Fig. 4), and a direct estimate from data of the average jet-quenching effect at detector level. The extrapolation to peripheral collisions (centrality $>$ 60%) shows that, in the absence of final-state medium effects, the data-to-simulation ratio is compatible with unity, indicating good agreement of the simulation with data. For central collisions (centrality $<$ 10%), this ratio is reduced by $>$20%, given that medium effects are absent in the simulation.

The training of UPART has been performed considering separate classes for UE jets and jets from the hard process. This results in an inefficiency of the algorithm in selecting UE jets. Using Z + jet events, the UPART efficiencies have been measured separately for UE and jets recoiling against the Z boson. In the regime considered in the analysis, UPART is fully efficient for recoil jets, while being inefficient for UE jets with $p_\mathrm{T} < 70\,\mathrm{GeV}$. Data-to-MC scale factors for these efficiencies are parameterized as functions of the collision centrality and the uncorrected jet p_T, and are applied to the baseline simulation as event weights to more accurately reproduce the UPART performance observed in data. The scale factors account for up to 20% differences between data and MC simulations, being larger for UE jets and in the 0–10% centrality bin. In the analysis, the simulated jet p_T is additionally corrected using the measured $\langle x_\mathrm{j} \rangle$ profile. The uncertainties associated with this procedure range from 2 to 20%, depending on the centrality and p_T bins and jet origin.

The adopted procedure is expected to provide a consistent description of the jets in data; any

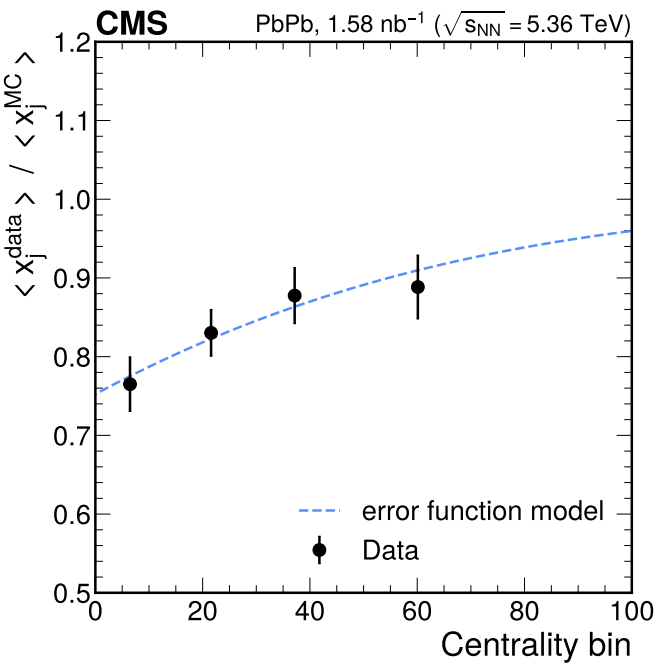


Figure 4: Ratio of the average $\langle x_j \rangle$ detector-level distributions measured in data over simulation as a function of the collision centrality with a fit to an error function (blue dashed curve) superimposed.

inconsistency would manifest as significant discrepancies in the number of reconstructed inclusive and/or bottom-quark jets. We therefore validate the approach by fitting the jet and b jet multiplicities in Z boson events. The results of these fits are displayed in Fig. 5 for central (left) and semicentral (right) PbPb collisions, and show a very good description of the inclusive jet (upper) and b jet (lower) multiplicities.

5 Background estimation

After the selection of dilepton pairs as described in Section 4, two main sources of background remain: DY production, which enters into the SF categories, and nonprompt leptons, which contribute mainly to the DF category.

The normalization of the DY background is left to float freely in the signal extraction fit described in Section 6. Prior to the fit, the counting of on-Z events shows good agreement between data and expectations within the uncertainties in the integrated luminosity and theoretical cross section. The data/theory ratios amount to $1.08 \pm 0.04\,(\text{stat})$ for the $\mathrm{e^+e^-}$ and $1.09 \pm 0.04\,(\text{stat})$ for the $\mu^+\mu^-$ channels. As illustrated in Section 6, good agreement is found between the measurements and the theoretical predictions in the BDT regions where DY production is expected to dominate.

The second main source of background is nonprompt and misidentified leptons from multijet QCD events. Given the large cross section for the production of heavy-flavor jets, the probability for these processes to mimic a $\mathrm{t\bar{t}}$ dilepton event is not necessarily negligible for the working points used for identification and isolation of the lepton candidates. However, when pairing two leptons in the event, their properties are expected to be mostly uncorrelated with each other, particularly if the leptons had their origin in different partonic interactions. This back-

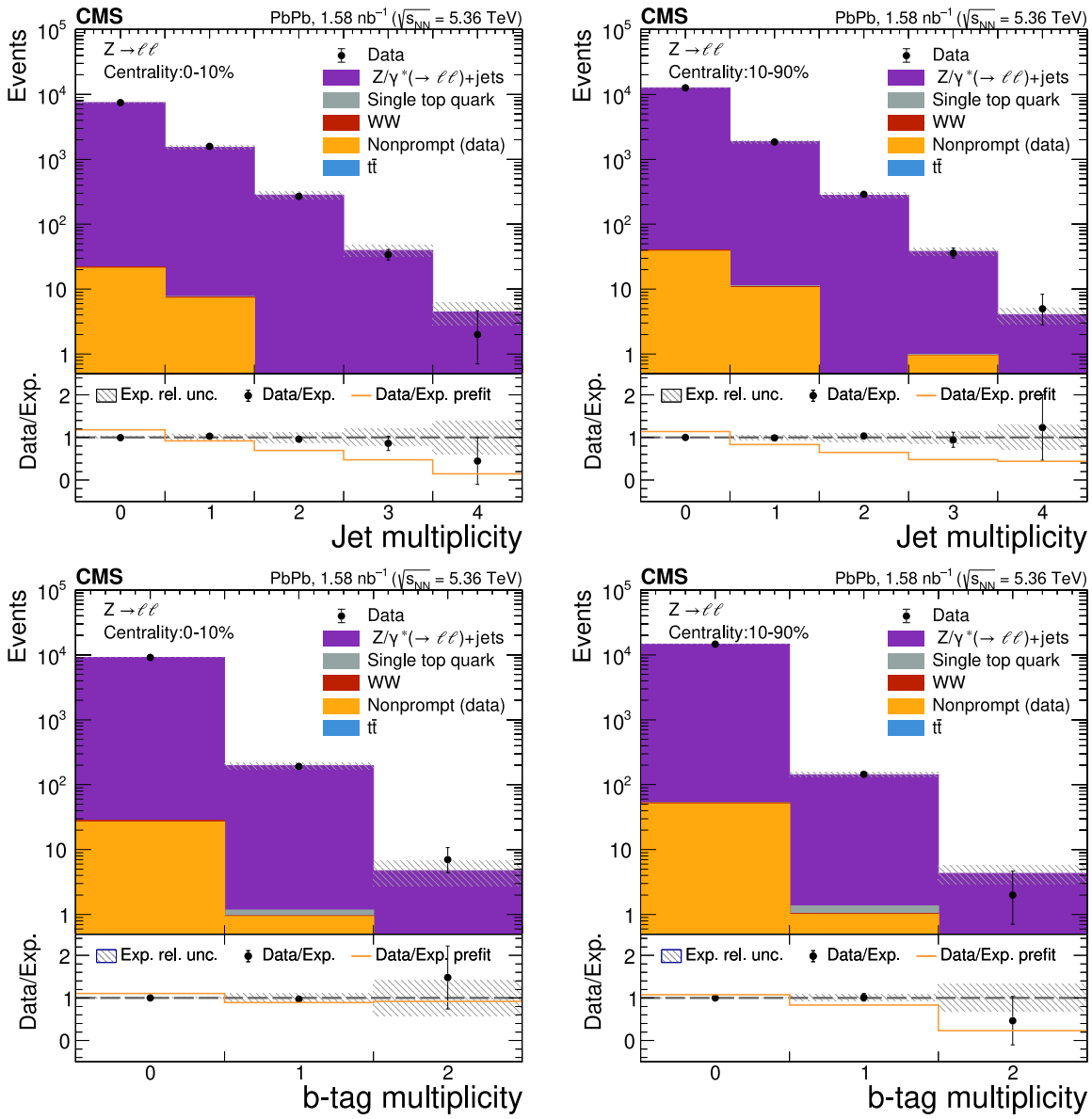


Figure 5: Multiplicities of inclusive (upper) and b-tagged (lower) jets in Z boson candidate events in the 0–10% (left) and 10–90% (right) centrality bins measured in the data (black markers) compared with the post-fit stacked model of the $t\bar{t}$ (blue), nonprompt (light orange), WW (red), single top quark (gray), and DY (violet) contributions. The lower panels show the data-to-expectation ratios before (orange lines) and after (black markers) the fit. The hatched band represents the post-fit uncertainty of the model in each bin. The last bins include the overflow entries.

ground is estimated based on an event-mixing technique which pairs leptons from different events as if they were produced in a single PbPb collision.

The selection of events to be mixed is performed by identifying the nearest neighbors in the three-dimensional space defined by the centrality, $p_{\mathrm{T}}(\ell\ell)$, and $m(\ell\ell)$ bins. The distances between events are evaluated using a k-D tree algorithm, which efficiently partitions the phase space in these variables and retrieves the closest matches [47, 48]. For each event, four alternative dilepton candidates are constructed in this way, and the distribution of their kinematic variables is used to obtain an alternative estimate of the nonprompt (combinatorial) background contribution. The final estimate is an average of the four with the normalization assigned based on the number of SS events selected in each channel. This technique significantly improves the statistical uncertainty associated with this background. Using simulated events, the accuracy of this method has been tested and ascribed an intrinsic uncertainty of 20–40%, depending on the final state.

Finally, other less relevant backgrounds include single top quark and diboson (notably WW) processes. These backgrounds are irreducible and estimated from the corresponding MC simulations described in Section 3 with the relevant data-to-MC corrections applied to them.

6 Signal extraction

The $\mathrm{t\bar{t}}$ signal strength $\mu = \sigma_{\mathrm{meas}}/\sigma_{\mathrm{th}}$ (where σ_{meas} and σ_{th} are the measured and theoretical cross sections, respectively) is extracted from a fit to the BDT output of the $\mathrm{e^+e^-}$, $\mu^+\mu^-$ (SF/off-Z/OS), and $\mathrm{e^{\mp}}\mu^{\pm}$ (DF/OS) channels, analyzed in events with zero, one, or at least two b-tagged jets. Two additional categories ($\mathrm{Z} \to \mathrm{e^+e^-}$ and $\mathrm{Z} \to \mu^+\mu^-$ in the on-Z/OS class) are added to the fit to control the normalization of the DY background. In each category, the fit is performed to the BDT output in events with zero, one, or at least two b-tagged jets. The impact of the systematic uncertainties on the signal and background expectations, detailed below, is modeled through a set of dedicated nuisance parameters [49]. The fitted BDT distributions are displayed in Fig. 6. In addition to the signal strength and the corresponding breakdown of statistical and systematic uncertainties, the significance of the $\mathrm{t\bar{t}}$ process is also extracted. The statistical analysis is performed using the COMBINE tool [50] based on the ROOFIT [51] and ROOSTATS [52] frameworks. The best-fit signal strength and its approximate 68% confidence level (CL) interval are extracted following the procedure outlined in Section 3.2 of [53], while the significance (Z score) is evaluated using an asymptotic approximation and validated with pseudo-experiments [54]. The experimental uncertainties can affect the modeling of both signal and backgrounds in the fit. They can be broadly grouped into those associated with the selection and calibration of physics objects, and those arising from the background estimation, as discussed below.

The efficiency of the trigger and lepton selections is corrected for the differences between data and simulation using scale factors derived from events in the $\mathrm{Z} \to \ell^+\ell^-$ CRs. The uncertainties associated with these scale factors are propagated to the analysis by varying the event weights used in the simulation, resulting in different predictions for the cross sections for the signal, single top, and diboson processes. The difference between these alternative predictions and the nominal one is parameterized as a function of several nuisance parameters depending on the type of lepton and the associated efficiency (trigger, identification, or isolation).

The impact of jet reconstruction inefficiencies in regions where CMS subdetectors suffer from aging or malfunctioning components is evaluated. These areas are mapped in the η–ϕ plane, and simulated jets with hadronic activity inside them are removed from the event. The result-

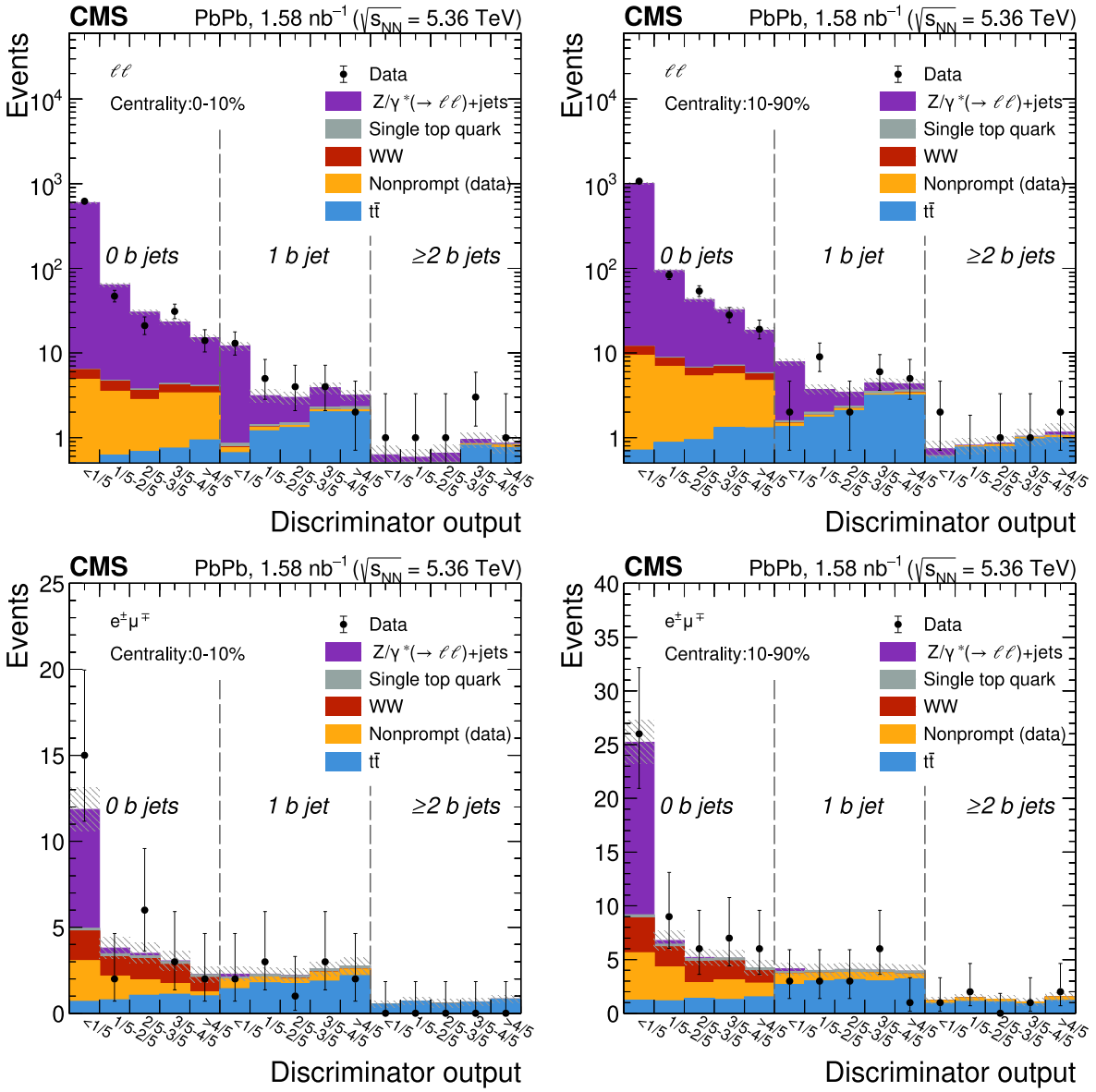


Figure 6: Distributions of the final BDT discriminator after the fit for the same-flavor $\ell\ell$ (upper) and different-flavor $e^{\mp}\mu^{\pm}$ (lower) channels. The discriminator output is shown for 0, 1, and $\geq$ 2 b-tagged jet events. The left (right) figures correspond to events reconstructed in the 0–10% (10–90%) centrality bin. The data (black markers) are compared with the stacked histograms corresponding to the $t\bar{t}$ signal (blue), and the nonprompt (light orange), WW (red), single top quark (gray), and DY (violet) background processes normalized to their post-fit expectations. The hatched gray bands show the total uncertainty in the predicted yields after the fit is performed.

ing differences in the BDT shapes, relative to the nominal simulation, are assigned as a systematic uncertainty. Additional sources of jet selection inefficiency may arise from the UPART application, as discussed in Section 4. To assess this effect, the data-to-simulation scale factors associated with the UPART efficiency are independently varied for UE jets and for jets matched to the hard process in the simulation. The corresponding variations in the BDT distributions are taken as a systematic uncertainty.

The impact of the jet energy scale uncertainty on the final observables is broken down into four main contributions: parton type, hadronization, process dependence, and uncertainty in the residual scale. The parton type uncertainty is estimated from simulation based on the different responses of b, and light-quark or gluon jets with respect to the mixed-flavor response. The hadronization uncertainty is evaluated from the difference in detector response obtained when using PYTHIA versus HERWIG 7 [55, 56] as parton shower and hadronization models. The process-dependent uncertainties result from the fact that UPART has been trained using $\mathrm{t\bar{t}}$ events, and it may thereby exhibit residual response differences when applied to other final states with different jet kinematics. This effect is evaluated from the jet response in the $\mathrm{Z}+$ jets MC sample. Finally, the residual scale uncertainty is subdivided into two sources: jet quenching and extrapolation to the vacuum or peripheral collision regime. Both are estimated from the average x_{j} ratio measured in data over the MC prediction (Fig. 4). The deviation from unity when extrapolating the relative response to peripheral events is considered as a $\approx$5% systematic uncertainty. The systematic uncertainty associated with jet quenching is evaluated by comparing the final observables with and without applying the parameterized energy loss shown in Fig. 4 on a jet-by-jet basis in the simulation. This procedure leads to a substantial loss of efficiency for reconstructing jets with $p_{\mathrm{T}} > 30\,\mathrm{GeV}$, thereby affecting the jet multiplicity in the b-tagged analysis. Finally, the impact of b tagging on the predicted distributions shown in Fig. 6 is assessed by varying the b tagging working point, i.e. using loose or tight instead of intermediate, such that the signal efficiency changes by $\pm$10%. These variations correspond to an expected change of the misidentification rate by more than a factor of two [44].

Beyond the uncertainties affecting the reconstruction of physics objects, the normalization of the event yields is impacted by a 6.4% uncertainty in the total PbPb integrated luminosity obtained from a preliminary analysis of van der Meer scan data collected during the PbPb run, following the same methodology of Ref. [57].

All simulated signal and background samples are affected by the experimental uncertainties described above. In the signal extraction fit, these uncertainties are treated as fully correlated between signal and background processes, with the exception of the b tagging uncertainties. The latter are kept uncorrelated to reflect the different parton type and kinematics between the on-Z CR and the $\mathrm{t\bar{t}}$ signal region. Theoretical uncertainties from missing higher-order corrections in the ME predictions are evaluated by varying the μ_{F} and μ_{R} scales within factors of two (excluding variations in opposite directions). The nuisance parameters associated with these scale uncertainties are treated as uncorrelated between the background and signal samples. The normalization of the dominant DY background is left unconstrained in the fit, but an additional model uncertainty is introduced from the difference between the shape of the POWHEG and MADGRAPH5_aMC@NLO predictions. For the nonprompt-lepton background, uncertainties arise from its normalization (20–40%), and from differences in shape between the event-mixing method and the SS and nonisolated sidebands. An uncertainty of 30% in the absolute normalization of other backgrounds (single top and W W) has been included in the fit. Statistical uncertainties in the simulated background differential cross sections are also incorporated via a Barlow–Beeston "lite" treatment [58].

Finally, the signal MC samples include two classes of modeling uncertainties. First, differences between the signal BDT shapes predicted by POWHEG and MADGRAPH5_aMC@NLO are included as a ME generator uncertainty. Although this variation is nominally one-sided, a symmetrized uncertainty is used in the statistical analysis. Additional modeling uncertainties are introduced by varying the top quark mass by $\pm 1\,\text{GeV}$ (implemented through generator-level reweighting using relativistic Breit–Wigner ratios) and by modifying the top quark p_{T} spectrum through an empirical reweighting that reproduces the softer p_{T} distribution observed in the pp data [59]. Second, uncertainties from the parton densities are evaluated by reweighting the $\mathrm{t\bar{t}}$ events using all eigenvectors of the EPPS21_nlo set—a total of 106 variations—and propagating the resulting changes in the BDT output. The final nPDF plus α_{S} uncertainties are determined following the PDF4LHC prescription [60].

7 Results

The distributions of the dilepton BDT discriminators in the different b-tagged jet multiplicity categories are shown in Fig. 6. In all plots, the event yields of the processes are normalized to the values determined by the fit. Fair agreement between data and post-fit expectations is obtained in the regions dominated by the backgrounds. In high-purity signal regions, the statistical fluctuations remain sizeable. The BDT discriminator exhibits strong separating power between the signal and the various background processes throughout all spectra. The inclusion of the b tag multiplicity yields additional discriminating power, improving separation even in low-purity regions.

Through the data fitting procedure described in Section 6, the $\mathrm{t\bar{t}}$ yield is extracted with a signal strength of $\mu(\mathrm{t\bar{t}}) = 0.93^{+0.15}_{-0.14}\,(\text{stat})^{+0.14}_{-0.12}\,(\text{syst})$, corresponding to an observed significance exceeding five standard deviations relative to the background-only hypothesis [61]. The likelihood scan is shown in Fig. 7. The statistical uncertainty remains slightly larger than the systematic component. Systematic uncertainties, particularly those associated with object efficiencies and background modeling, are expected to decrease further as larger data samples become available in the future.

The main systematic uncertainties arise from the b tagging, integrated luminosity, and the normalization in the DY and nonprompt-lepton backgrounds. The impact of each source of systematic uncertainty in the extracted signal strength is quantified by evaluating the shift induced when the corresponding nuisance parameter is varied up or down by its post-fit uncertainty [50]. Figure 8 shows the resulting impact magnitudes for the dominant sources of uncertainty. The p-value associated with the goodness-of-fit is estimated to be 10%. Several cross-checks have been performed to assess the robustness of the fit, including separate analyses of the different final states, the omission of b tagging requirements, the exclusion of the Z boson CRs from the fit, and measurements performed in exclusive centrality categories. In all cases, the results are found to be compatible with the signal strength derived in the default analysis.

From the signal strength, a cross section $\sigma_{\mathrm{t\bar{t}}} = 3.42^{+0.54}_{-0.51}\,(\text{stat})^{+0.50}_{-0.43}\,(\text{syst})\,\mu\text{b}$ is derived, which is in agreement with the pQCD predictions at NNLO + NNLL accuracy. The DY cross section, measured in a phase space where $m(\ell\ell) > 10\,\text{GeV}$, is found to be $\sigma_{\mathrm{DY}} = 397 \pm 3\,(\text{stat})^{+27}_{-25}\,(\text{syst})\,\mu\text{b}$, with uncertainties dominated by the PbPb integrated luminosity, also in agreement with the theoretical expectations ($\sigma^{\mathrm{th}}_{\mathrm{DY}} = 370\,\mu\text{b}$ for the central NNLO value obtained with EPPS21_nlo). Partial reduction of some of the main systematic uncertainties, such as the integrated luminosity and lepton efficiencies, can be achieved by measuring the ratio

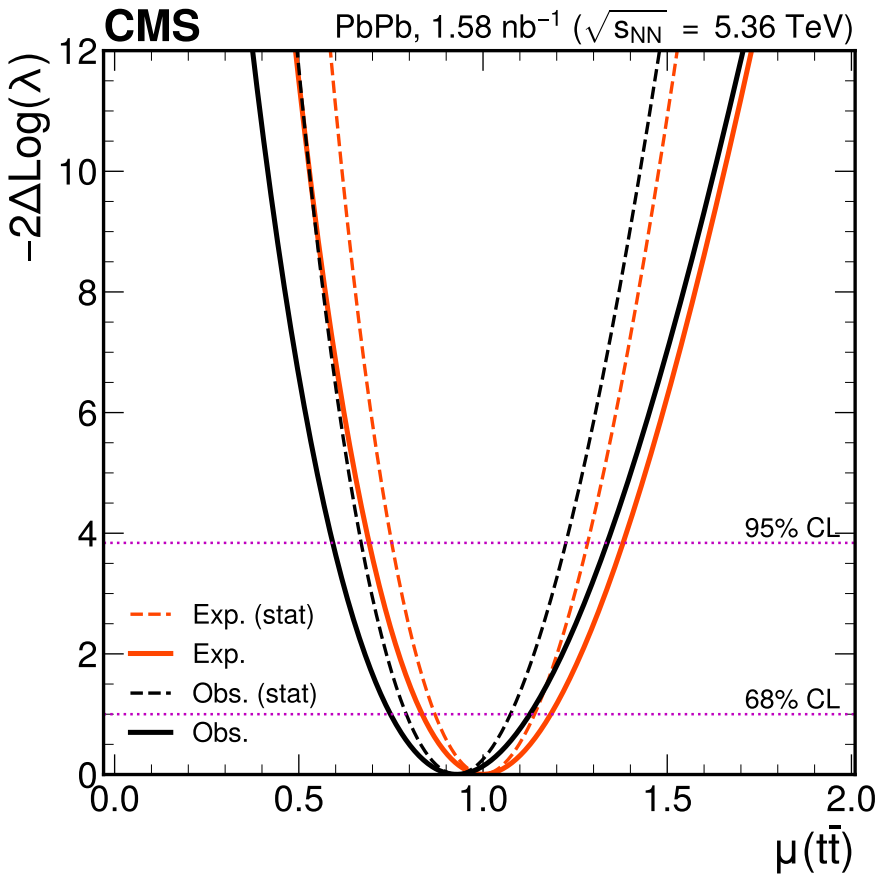


Figure 7: Scan of the profile likelihood as a function of the $t\bar{t}$ signal strength. The expected (orange) and observed (black) scans are displayed with (solid curve) and without (dashed curve) accounting for systematic uncertainties. The horizontal dashed lines indicate the likelihood values used to extract the 68% and 95% CL intervals on the parameter of interest.

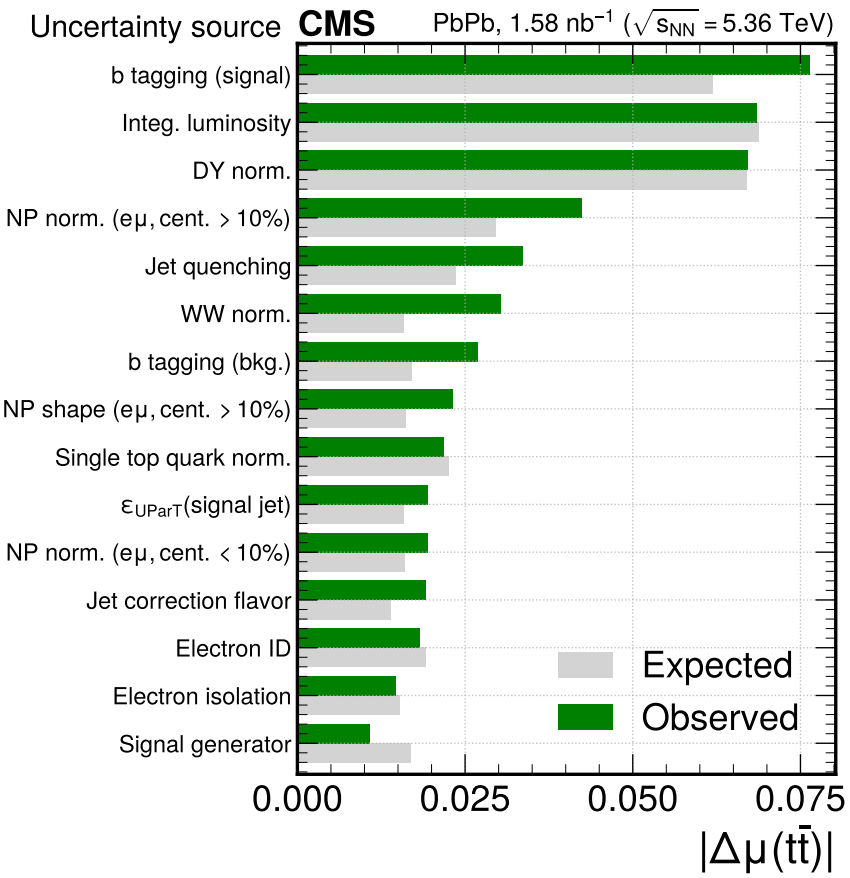


Figure 8: Impact of systematic uncertainties on the fitted $t\bar{t}$ signal strength parameter. The systematic uncertainties are listed in decreasing order of their impact on the signal strength.

of the $\mathrm{t\bar{t}}$ over the DY cross sections. In addition, given that $\mathrm{t\bar{t}}$ is preferentially produced via gluon-gluon fusion, whereas DY pairs through quark-antiquark annihilation, this ratio directly probes the relative gluon and quark content of the nuclear PDFs. The ratio of the two cross sections is evaluated in the full phase space for the $\mathrm{t\bar{t}}$ process and for pair masses $m(\ell\ell) > 10\,\mathrm{GeV}$ for the DY process. The extrapolation of the visible signal strength of each process to the full phase space results in an intrinsic uncertainty of $^{+2.8\%}_{-3.1\%}$, estimated using NLO pQCD predictions. The measured ratio amounts to $R_{\mathrm{t\bar{t}/DY}} = 0.0086^{+0.0014}_{-0.0013}\,(\mathrm{stat})^{+0.0011}_{-0.0010}\,(\mathrm{syst})$ in agreement with the theoretical ratio at NNLO accuracy, $R^{\mathrm{th}}_{\mathrm{t\bar{t}/DY}} = 0.0108^{+0.0026}_{-0.0023}$ (nPDF+scales), obtained with the EPPS21_nlo nPDFs using TOP++ and DYTURBO [62] for the numerator and denominator, respectively.

Figure 9 compares the experimental $\mathrm{t\bar{t}}$ (upper) and DY (middle) cross section as well as $R_{\mathrm{t\bar{t}/DY}}$ ratio (lower) with the theoretical predictions obtained at NLO or NNLO pQCD accuracy (as indicated in parentheses in the legends) using different PDFs: EPPS21_nlo [23], nNNPDF10_(n)nlo [63], nNNPDF30_nlo [64], and TUJU21_(n)nlo [65] nuclear sets, as well as NNPDF30_nlo [66], and CT18_(n)nlo proton PDF sets. The statistical and total experimental uncertainties are shown as orange and blue bands in the plots, respectively. The black error bars denote the total theoretical uncertainty; the inner bars indicate the contribution from nPDF plus parametric (α_{S} and m_{t}) uncertainties. Overall, the measurements are in good agreement with the theoretical predictions within uncertainties for all observables. Considering the theoretical predictions for the $\mathrm{t\bar{t}}$ production cross sections, several features are noteworthy. First, for any given (n)PDF set, the NNLO predictions are larger than their NLO counterparts. Second, again for the same (n)PDF input, the NNLO calculations exhibit reduced uncertainties—particularly those associated with theoretical scale variations—relative to the NLO results. Third, the cross sections obtained using proton PDFs are a few percent smaller than those derived with nuclear PDFs, reflecting a mild antishadowing effect in the nuclear parton densities [3]. Finally, the substantially larger uncertainties of nNNPDF1.0 compared with the more recent nNNPDF3.0 set are expected, since the former relies solely on legacy fixed-target nuclear data, whereas the latter incorporates a broad range of modern LHC measurements. Although the current experimental precision of the $\mathrm{t\bar{t}}$ cross section does not yet allow discrimination among predictions based on different nPDF sets, it is worth noting that the corresponding theoretical uncertainties are of comparable magnitude to the combined measurement presented here. In contrast, for the DY cross section and the $R_{\mathrm{t\bar{t}/DY}}$ observable, the uncertainties on the theoretical predictions are, in several cases, larger than the experimental ones. These measurements are therefore expected to provide new and meaningful constraints in future global nPDF fits, particularly by probing kinematic regions that have not been accessible in previous analyses.

In addition, the $\mathrm{t\bar{t}}$ and DY cross sections, as well as their ratio, are measured separately for 0–10% central and 10–90% semicentral PbPb collisions. Table 1 summarizes all the experimental results obtained. Figure 10 shows the different observables measured in the three PbPb centrality selections (10–90%, 0–10% and inclusive) compared with the corresponding theoretical predictions obtained at NNLO + NNLL pQCD accuracy with the EPPS21_nlo set. In all cases, the measurements are consistent with the pQCD NNLO predictions. The ratio $R_{\mathrm{t\bar{t}/DY}}$ is observed to be independent of the centrality, as expected.

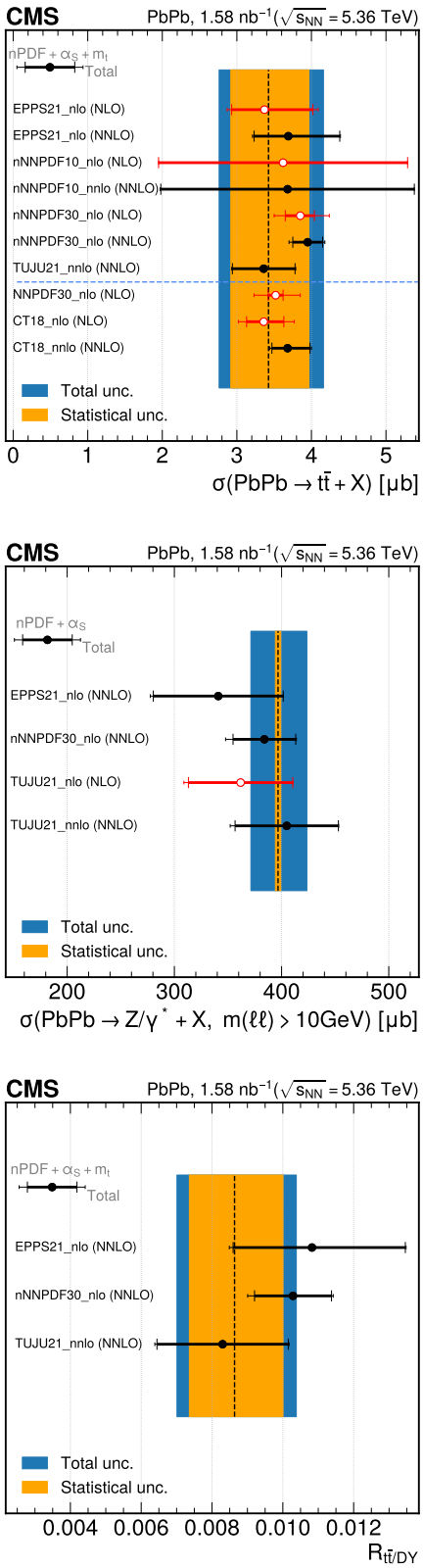


Figure 9: Experimental measurements (colored bands) of the $t\bar{t}$ cross section (upper), DY cross section (middle), and $R_{t\bar{t}/DY}$ ratio (lower) in inclusive PbPb collisions at $\sqrt{s_{NN}} = 5.36\,TeV$ compared with the corresponding NLO (red bars) or NNLO + NNLL (black bars) theoretical predictions obtained with the EPPS21_nlo, nNNPDF10_(n)nlo, nNNPDF30_nlo, and TUJU21_(n)nlo nPDF sets. The error bars represent the theoretical uncertainties, and the blue (orange) area shows the total (statistical) uncertainties of the measurements. In the upper plot a dashed line separates the theory predictions obtained with nuclear PDFs (above the line) from those with the proton PDFs (below the line).

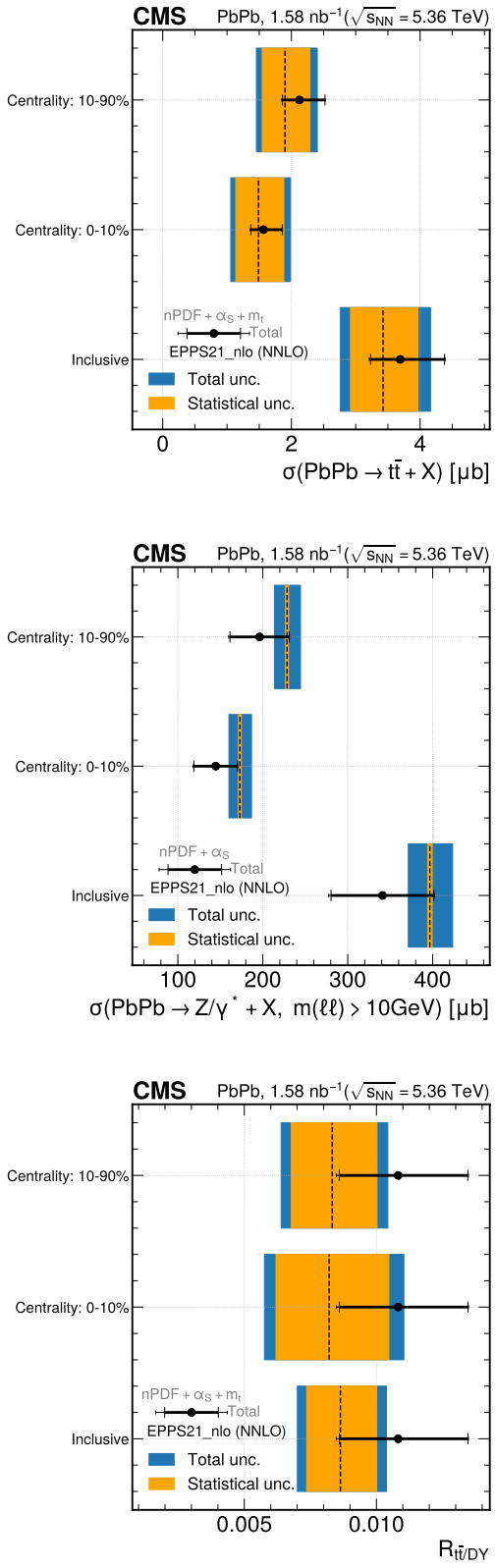


Figure 10: Experimental measurements (colored bands) of the $t\bar{t}$ cross section (upper), DY cross section (middle), and $R_{t\bar{t}/DY}$ ratio (lower) in semicentral (10–90%), central (0–10%), and inclusive PbPb collisions at $\sqrt{s_{NN}} = 5.36\,\text{TeV}$ compared with the corresponding NNLO + NNLL theoretical predictions (black markers with error bars) obtained with the EPPS21_nlo [23] nPDF set. The blue (orange) bands indicate the total (statistical) uncertainties of the measured observables, whereas the error bars represent the uncertainties in the theory calculations.

Table 1: Measured $\mathrm{t\bar{t}}$ cross section, DY cross section, and $R_{\mathrm{t\bar{t}}/\mathrm{DY}}$ ratio for three different PbPb centrality selections. For each measurement, the statistical and systematic uncertainty components are shown separately.

Centrality bin	$\sigma_{\mathrm{t\bar{t}}}$ [μb]	σ_{DY} [μb]	$R_{\mathrm{t\bar{t}}/\mathrm{DY}}$
Inclusive	$3.42^{+0.54}_{-0.51}\,(\mathrm{stat})^{+0.50}_{-0.43}\,(\mathrm{syst})$	$397 \pm 3\,(\mathrm{stat})^{+27}_{-25}\,(\mathrm{syst})$	$0.0086^{+0.0014}_{-0.0013}\,(\mathrm{stat})^{+0.0011}_{-0.0010}\,(\mathrm{syst})$
0–10 %	$1.49^{+0.40}_{-0.35}\,(\mathrm{stat})^{+0.31}_{-0.25}\,(\mathrm{syst})$	$173.0 \pm 1.7\,(\mathrm{stat})^{+13.6}_{-12.7}\,(\mathrm{syst})$	$0.0082^{+0.0023}_{-0.0020}\,(\mathrm{stat})^{+0.0017}_{-0.0014}\,(\mathrm{syst})$
10–90 %	$1.90^{+0.40}_{-0.35}\,(\mathrm{stat})^{+0.32}_{-0.27}\,(\mathrm{syst})$	$228.6 \pm 1.8\,(\mathrm{stat})^{+15.7}_{-14.8}\,(\mathrm{syst})$	$0.0083^{+0.0017}_{-0.0015}\,(\mathrm{stat})^{+0.0012}_{-0.0011}\,(\mathrm{syst})$

8 Summary

The first measurement of the inclusive production of top quark pairs ($\mathrm{t\bar{t}}$) in lead-lead (PbPb) collisions at a nucleon-nucleon center-of-mass energy of $\sqrt{s_{\mathrm{NN}}} = 5.36\,\mathrm{TeV}$ has been presented, extending earlier studies performed at lower collision energies. The analysis is based on dilepton events selected from the 2023 dataset recorded by the CMS experiment, corresponding to an integrated luminosity of $1.58\,\mathrm{nb}^{-1}$. Several improvements have been implemented—including enhanced electron identification and lepton isolation, refined heavy-flavor jet identification, and a dedicated calibration of the b jet energy scale—which collectively provide a substantial gain in precision compared with previous analyses.

The cross sections $\sigma_{\mathrm{t\bar{t}}} = 3.42^{+0.54}_{-0.51}\,(\mathrm{stat})^{+0.50}_{-0.43}\,(\mathrm{syst})\,\mu\mathrm{b}$, and $\sigma_{\mathrm{DY}} = 397 \pm 3\,(\mathrm{stat})^{+27}_{-25}\,(\mathrm{syst})\,\mu\mathrm{b}$ for the Drell–Yan process, along with their ratio $R_{\mathrm{t\bar{t}/DY}} = 0.0086^{+0.0014}_{-0.0013}\,(\mathrm{stat})^{+0.0011}_{-0.0010}\,(\mathrm{syst})$, have been measured. The $\sigma_{\mathrm{t\bar{t}}}$ and $R_{\mathrm{t\bar{t}/DY}}$ measurements have total uncertainties of ≈20% and are consistent with perturbative quantum chromodynamics calculations at next-to-next-to-leading-order accuracy obtained using different nuclear parton distribution functions. Results for central and semicentral PbPb collisions are also reported for the first time to examine the dependence of the top quark yields on the collision impact parameter. Combined with the higher collision energy and the larger data samples anticipated for the remainder of Run 3, these developments firmly establish top quark production as a future probe of initial- and final-state effects in heavy ions.

Acknowledgments

We congratulate our colleagues in the CERN accelerator departments for the excellent performance of the LHC and thank the technical and administrative staffs at CERN and at other CMS institutes for their contributions to the success of the CMS effort. In addition, we gratefully acknowledge the computing centers and personnel of the Worldwide LHC Computing Grid and other centers for delivering so effectively the computing infrastructure essential to our analyses. Finally, we acknowledge the enduring support for the construction and operation of the LHC, the CMS detector, and the supporting computing infrastructure provided by the following funding agencies: SC (Armenia), BMBWF and FWF (Austria); FNRS and FWO (Belgium); CNPq, CAPES, FAPERJ, FAPERGS, and FAPESP (Brazil); MES and BNSF (Bulgaria); CERN; CAS, MoST, and NSFC (China); MINCIENCIAS (Colombia); MSES and CSF (Croatia); RIF (Cyprus); SENESCYT (Ecuador); ERC PRG and PSG, TARISTU24-TK10 and MoER TK202 (Estonia); Academy of Finland, MEC, and HIP (Finland); CEA and CNRS/IN2P3 (France); SRNSF (Georgia); BMFTR, DFG, and HGF (Germany); GSRI (Greece); MATE and NKFIH (Hungary); DAE and DST (India); IPM (Iran); SFI (Ireland); INFN (Italy); MSIT and NRF (Republic of Korea); MES (Latvia); LMTLT (Lithuania); MOE and UM (Malaysia); BUAP, CINVESTAV, CONACYT, LNS, SEP, and UASLP-FAI (Mexico); MOS (Montenegro); MBIE (New Zealand); PAEC (Pakistan); MSHE, NSC, and NAWA (Poland); FCT (Portugal); MESTD (Serbia); MICIU/AEI and PCTI (Spain); MOSTR (Sri Lanka); Swiss Funding Agencies (Switzerland); MST (Taipei); MHESI (Thailand); TUBITAK and TENMAK (Türkiye); NASU (Ukraine); STFC (United Kingdom); DOE and NSF (USA).

Individuals have received support from the Marie-Curie program and the European Research Council and Horizon 2020 Grant, contract Nos. 675440, 724704, 752730, 758316, 765710, 824093, 101115353, 101002207, 101001205, and COST Action CA16108 (European Union); the Leventis Foundation; the Alfred P. Sloan Foundation; the Alexander von Humboldt Foundation; the Science Committee, project no. 22rl-037 (Armenia); the Fonds pour la Formation à la Recherche dans l'Industrie et dans l'Agriculture (FRIA) and Fonds voor Weten-

schappelijk Onderzoek contract No. 1228724N (Belgium); the Beijing Municipal Science & Technology Commission, No. Z191100007219010, the Fundamental Research Funds for the Central Universities, the Ministry of Science and Technology of China under Grant No. 2023YFA1605804, the Natural Science Foundation of China under Grant No. 12535004, and USTC Research Funds of the Double First-Class Initiative No. YD2030002017 (China); the Ministry of Education, Youth and Sports (MEYS) of the Czech Republic; the Shota Rustaveli National Science Foundation, grant FR-22-985 (Georgia); the Deutsche Forschungsgemeinschaft (DFG), among others, under Germany's Excellence Strategy – EXC 2121 "Quantum Universe" – 390833306, and under project number 400140256 - GRK2497; the Hellenic Foundation for Research and Innovation (HFRI), Project Number 2288 (Greece); the Hungarian Academy of Sciences, the New National Excellence Program - ÚNKP, the NKFIH research grants K 131991, K 138136, K 143460, K 143477, K 147557, K 146913, K 146914, K 147048, TKP2021-NKTA-64, and 2025-1.1.5-NEMZ_KI-2025-00004, and MATE KKP and KKPCs Research Excellence and Flagship Research Groups grants (Hungary); the Council of Science and Industrial Research, India; ICSC – National Research Center for High Performance Computing, Big Data and Quantum Computing, FAIR – Future Artificial Intelligence Research, and CUP I53D23001070006 (Mission 4 Component 1), funded by the NextGenerationEU program, the Italian Ministry of University and Research (MUR) under Bando PRIN 2022 – CUP I53C24002390006, PRIN PRIMULA 2022RBYK7T (Italy); the Latvian Council of Science; the Ministry of Science and Higher Education, project no. 2022/WK/14, and the National Science Center, contracts Opus 2021/41/B/ST2/01369, 2021/43/B/ST2/01552, 2023/49/B/ST2/03273, and the NAWA contract BPN/PPO/2021/1/00011 (Poland); the Fundação para a Ciência e a Tecnologia (Portugal); the National Priorities Research Program by Qatar National Research Fund; MICIU/AEI/10.13039/501100011033, ERDF/EU, "European Union NextGenerationEU/PRTR", projects PID2022-142604OB-C21, PID2022-139519OB-C21, PID2023-147706NB-I00, PID2023-148896NB-I00, PID2023-146983NB-I00, PID2023-147115NB-I00, PID2023-148418NB-C41, PID2023-148418NB-C42, PID2023-148418NB-C43, PID2023-148418NB-C44, PID2024-158190NB-C22, RYC2021-033305-I, RYC2024-048719-I, CNS2023-144781, CNS2024-154769 and Plan de Ciencia, Tecnología e Innovación de Asturias, Spain; the Chulalongkorn Academic into Its 2nd Century Project Advancement Project, the National Science, Research and Innovation Fund program IND_FF_68_369_2300_097, and the Program Management Unit for Human Resources & Institutional Development, Research and Innovation, grant B39G680009 (Thailand); the Eric & Wendy Schmidt Fund for Strategic Innovation through the CERN Next Generation Triggers project under grant agreement number SIF-2023-004; the Kavli Foundation; the Nvidia Corporation; the SuperMicro Corporation; the Welch Foundation, contract C-1845; and the Weston Havens Foundation (USA).

References

[1] CMS Collaboration, "Stairway to discovery: a report on the CMS programme of cross section measurements from millibarns to femtobarns", *Phys. Rept.* **1115** (2025) 3, doi:10.1016/j.physrep.2024.11.005, arXiv:2405.18661.

[2] ATLAS Collaboration, "Climbing to the top of the ATLAS 13 TeV data", *Phys. Rept.* **1116** (2025) 127, doi:10.1016/j.physrep.2024.12.004, arXiv:2404.10674.

[3] D. d'Enterria, K. Krajczár, and H. Paukkunen, "Top-quark production in proton–nucleus and nucleus–nucleus collisions at LHC energies and beyond", *Phys. Lett. B* **746** (2015) 64, doi:10.1016/j.physletb.2015.04.044, arXiv:1501.05879.

[4] L. Apolinário, J. G. Milhano, G. P. Salam, and C. A. Salgado, "Probing the time structure of the quark-gluon plasma with top quarks", *Phys. Rev. Lett.* **120** (2018) 232301, doi:10.1103/PhysRevLett.120.232301, arXiv:1711.03105.

[5] Particle Data Group, S. Navas et al., "Review of particle physics", *Phys. Rev. D* **110** (2024) 030001, doi:10.1103/PhysRevD.110.030001.

[6] CMS Collaboration, "Measurement of differential $\mathrm{t\bar{t}}$ production cross sections in the full kinematic range using lepton+jets events from proton-proton collisions at $\sqrt{s} = 13$ TeV", *Phys. Rev. D* **104** (2021) 092013, doi:10.1103/PhysRevD.104.092013, arXiv:2108.02803.

[7] CMS Collaboration, "Measurement of the $\mathrm{t\bar{t}}$ production cross section, the top quark mass, and the strong coupling constant using dilepton events in pp collisions at $\sqrt{s} = 13$ TeV", *Eur. Phys. J. C* **79** (2019) 368, doi:10.1140/epjc/s10052-019-6863-8, arXiv:1812.10505.

[8] CMS Collaboration, "Observation of top quark production in proton-nucleus collisions", *Phys. Rev. Lett.* **119** (2017) 242001, doi:10.1103/PhysRevLett.119.242001, arXiv:1709.07411.

[9] ATLAS Collaboration, "Observation of $\mathrm{t\bar{t}}$ production in the lepton+jets and dilepton channels in p+Pb collisions at $\sqrt{s_{\mathrm{NN}}} = 8.16$ TeV with the ATLAS detector", *JHEP* **11** (2024) 101, doi:10.1007/JHEP11(2024)101, arXiv:2405.05078.

[10] CMS Collaboration, "Evidence for top quark production in nucleus-nucleus collisions", *Phys. Rev. Lett.* **125** (2020) 222001, doi:10.1103/PhysRevLett.125.222001, arXiv:2006.11110.

[11] ATLAS Collaboration, "Observation of $\mathrm{t\bar{t}}$ production in Pb+Pb collisions at $\sqrt{s_{\mathrm{NN}}} = 5.02$ TeV with the ATLAS detector", *Phys. Rev. Lett.* **134** (2025) 142301, doi:10.1103/PhysRevLett.134.142301, arXiv:2411.10186.

[12] HEPData record for this analysis, 2026. doi:10.17182/hepdata.168317.

[13] CMS Collaboration, "The CMS experiment at the CERN LHC", *JINST* **3** (2008) S08004, doi:10.1088/1748-0221/3/08/S08004.

[14] CMS Collaboration, "Development of the CMS detector for the CERN LHC Run 3", *JINST* **19** (2024), no. 05, P05064, doi:10.1088/1748-0221/19/05/P05064, arXiv:2309.05466.

[15] CMS Collaboration, "Performance of the CMS level-1 trigger in proton-proton collisions at $\sqrt{s} = 13$ TeV", *JINST* **15** (2020) P10017, doi:10.1088/1748-0221/15/10/P10017, arXiv:2006.10165.

[16] CMS Collaboration, "The CMS trigger system", *JINST* **12** (2017) P01020, doi:10.1088/1748-0221/12/01/P01020, arXiv:1609.02366.

[17] CMS Collaboration, "Performance of the CMS high-level trigger during LHC run 2", *JINST* **19** (2024) P11021, doi:10.1088/1748-0221/19/11/P11021, arXiv:2410.17038.

[18] CMS Collaboration, "Electron and photon reconstruction and identification with the CMS experiment at the CERN LHC", *JINST* **16** (2021) P05014, doi:10.1088/1748-0221/16/05/P05014, arXiv:2012.06888.

[19] CMS Collaboration, "Performance of the CMS muon detector and muon reconstruction with proton-proton collisions at $\sqrt{s} = 13$ TeV", *JINST* **13** (2018) P06015, doi:10.1088/1748-0221/13/06/P06015, arXiv:1804.04528.

[20] CMS Collaboration, "Description and performance of track and primary-vertex reconstruction with the CMS tracker", *JINST* **9** (2014) P10009, doi:10.1088/1748-0221/9/10/P10009, arXiv:1405.6569.

[21] CMS Collaboration, "Status of zero degree calorimeter for the CMS experiment", *AIP Conf. Proc.* **867** (2006) 258, doi:10.1063/1.2396962, arXiv:nucl-ex/0608052.

[22] CMS Collaboration, "Particle-flow reconstruction and global event description with the CMS detector", *JINST* **12** (2017) P10003, doi:10.1088/1748-0221/12/10/P10003, arXiv:1706.04965.

[23] K. J. Eskola, P. Paakkinen, H. Paukkunen, and C. A. Salgado, "EPPS21: a global QCD analysis of nuclear PDFs", *Eur. Phys. J. C* **82** (2022) 413, doi:10.1140/epjc/s10052-022-10359-0, arXiv:2112.12462.

[24] T.-J. Hou et al., "New CTEQ global analysis of quantum chromodynamics with high-precision data from the LHC", *Phys. Rev. D* **103** (2021) 014013, doi:10.1103/PhysRevD.103.014013, arXiv:1912.10053.

[25] T. Sjöstrand et al., "An introduction to PYTHIA 8.2", *Comput. Phys. Commun.* **191** (2015) 159, doi:10.1016/j.cpc.2015.01.024, arXiv:1410.3012.

[26] CMS Collaboration, "Extraction and validation of a new set of CMS PYTHIA 8 tunes from underlying-event measurements", *Eur. Phys. J. C* **80** (2020) 4, doi:10.1140/epjc/s10052-019-7499-4, arXiv:1903.12179.

[27] I. P. Lokhtin et al., "Heavy ion event generator HYDJET++ (HYDrodynamics plus JETs)", *Comput. Phys. Commun.* **180** (2009) 779, doi:10.1016/j.cpc.2008.11.015, arXiv:0809.2708.

[28] D. d'Enterria and C. Loizides, "Progress in the Glauber model at collider energies", *Ann. Rev. Nucl. Part. Sci.* **71** (2021) 315, doi:10.1146/annurev-nucl-102419-060007, arXiv:2011.14909.

[29] GEANT4 Collaboration, "GEANT4—a simulation toolkit", *Nucl. Instrum. Meth. A* **506** (2003) 250, doi:10.1016/S0168-9002(03)01368-8.

[30] J. Alwall et al., "The automated computation of tree-level and next-to-leading order differential cross sections, and their matching to parton shower simulations", *JHEP* **07** (2014) 079, doi:10.1007/JHEP07(2014)079, arXiv:1405.0301.

[31] S. Frixione, P. Nason, and G. Ridolfi, "A positive-weight next-to-leading-order Monte Carlo for heavy flavour hadroproduction", *JHEP* **09** (2007) 126, doi:10.1088/1126-6708/2007/09/126, arXiv:0707.3088.

[32] R. Frederix and S. Frixione, "Merging meets matching in MC@NLO", *JHEP* **12** (2012) 061, doi:10.1007/JHEP12(2012)061, arXiv:1209.6215.

[33] M. Czakon, P. Fiedler, and A. Mitov, "Total top-quark pair-production cross section at hadron colliders through $\mathcal{O}(\alpha_s^4)$", *Phys. Rev. Lett.* **110** (2013) 252004, doi:10.1103/PhysRevLett.110.252004, arXiv:1303.6254.

[34] E. Re, "Single-top W t-channel production matched with parton showers using the POWHEG method", *Eur. Phys. J. C* **71** (2011) 1547, doi:10.1140/epjc/s10052-011-1547-z, arXiv:1009.2450.

[35] T. Chen and C. Guestrin, "XGBOOST: a scalable tree boosting system", in *22nd ACM SIGKDD Int. Conf. on Knowledge Discovery and Data Mining (KDD'16)*, p. 785. 2016. doi:10.1145/2939672.2939785.

[36] F. Pedregosa et al., "Scikit-learn: machine learning in Python", *J. Mach. Learn. Res.* **12** (2011) 2825, arXiv:1201.0490.

[37] M. Cacciari, G. P. Salam, and G. Soyez, "SoftKiller, a particle-level pileup removal method", *Eur. Phys. J. C* **75** (2015) 59, doi:10.1140/epjc/s10052-015-3267-2, arXiv:1407.0408.

[38] CMS Collaboration, "Measurement of light-by-light scattering and the Breit–Wheeler process, and search for axion-like particles in ultraperipheral PbPb collisions at $\sqrt{s_{\mathrm{NN}}} = 5.02$ TeV", *JHEP* **08** (2025) 006, doi:10.1007/JHEP08(2025)006, arXiv:2412.15413.

[39] R. Pezoa, L. Salinas, and C. Torres, "Explainability of high energy physics events classification using SHAP", *J. Phys. Conf. Ser.* **2438** (2023) 12082, doi:10.1088/1742-6596/2438/1/012082.

[40] T. Akiba et al., "OPTUNA: a next-generation hyperparameter optimization framework", in *25th ACM SIGKDD Int. Conf. on Knowledge Discovery and Data Mining (KDD'19)*, p. 2623. 2019. doi:10.1145/3292500.3330701.

[41] M. Cacciari, G. P. Salam, and G. Soyez, "The anti-k_{T} jet clustering algorithm", *JHEP* **04** (2008) 063, doi:10.1088/1126-6708/2008/04/063, arXiv:0802.1189.

[42] M. Cacciari, G. P. Salam, and G. Soyez, "FastJet user manual", *Eur. Phys. J. C* **72** (2012) 1896, doi:10.1140/epjc/s10052-012-1896-2, arXiv:1111.6097.

[43] CMS Collaboration, "A unified approach for jet tagging in Run 3 at $\sqrt{s} = 13.6$ TeV in CMS", CMS Detector Performance Summary CMS-DP-2024-066, 2024.

[44] CMS Collaboration, "Jet tagging performance in Run 3 PbPb collisions at 5.36 TeV in CMS", CMS Detector Performance Summary CMS-DP-2024-088, 2024.

[45] CMS Collaboration, "Performance of heavy-flavour jet identification in Lorentz-boosted topologies in proton-proton collisions at $\sqrt{s} = 13$ TeV", *JINST* **20** (2025) P11006, doi:10.1088/1748-0221/20/11/P11006, arXiv:2510.10228.

[46] M. J. Oreglia, "A study of the reactions $\psi' \to \gamma\gamma\psi$". PhD thesis, Stanford University, 1980. SLAC Report SLAC-R-236, see Appendix D.

[47] J. L. Bentley, "Multidimensional binary search trees used for associative searching", *Commun. ACM* **18** (1975) 509, doi:10.1145/361002.361007.

[48] R. Brun and F. Rademakers, "ROOT: an object-oriented data analysis framework", *Nucl. Instrum. Meth. A* **389** (1997) 81, doi:10.1016/S0168-9002(97)00048-X.

[49] J. S. Conway, "Incorporating nuisance parameters in likelihoods for multisource spectra", in *PHYSTAT 2011*, p. 115. 2011. arXiv:1103.0354. doi:10.5170/CERN-2011-006.115.

[50] CMS Collaboration, "The CMS statistical analysis and combination tool: Combine", *Comput. Softw. Big Sci.* **8** (2024) 19, doi:10.1007/s41781-024-00121-4, arXiv:2404.06614.

[51] W. Verkerke and D. Kirkby, "The RooFit toolkit for data modeling", in *Proc. 13th Int. Conf. on Computing in High Energy and Nuclear Physics (CHEP 2003): La Jolla CA, United States, March 24–28*. 2003. arXiv:physics/0306116.

[52] L. Moneta et al., "The RooStats project", in *Proc. 13th Int. Workshop on Advanced Computing and Analysis Techniques in Physics Research (ACAT 2010): Jaipur, India, February 22–27, 2010*. 2010. arXiv:1009.1003. doi:10.22323/1.093.0057.

[53] CMS Collaboration, "Precise determination of the mass of the Higgs boson and tests of compatibility of its couplings with the standard model predictions using proton collisions at 7 and 8 TeV", *Eur. Phys. J. C* **75** (2015) 212, doi:10.1140/epjc/s10052-015-3351-7, arXiv:1412.8662.

[54] L. Demortier, "p values and nuisance parameters", in *Statistical issues for LHC physics. Proceedings, Workshop, PHYSTAT-LHC, Geneva, Switzerland, June 27-29, 2007*, p. 23. 2008. doi:10.5170/CERN-2008-001.

[55] M. Bahr et al., "Herwig++ physics and manual", *Eur. Phys. J. C* **58** (2008) 639, doi:10.1140/epjc/s10052-008-0798-9, arXiv:0803.0883.

[56] J. Bellm et al., "Herwig 7.0/Herwig++ 3.0 release note", *Eur. Phys. J. C* **76** (2016) 196, doi:10.1140/epjc/s10052-016-4018-8, arXiv:1512.01178.

[57] CMS Collaboration, "Luminosity measurement for lead-lead collisions at $\sqrt{s_{_{\mathrm{NN}}}} = 5.02$ TeV in 2015 and 2018 at CMS", 2025. arXiv:2503.03946. Submitted to *Eur. Phys. J. C*.

[58] R. J. Barlow and C. Beeston, "Fitting using finite Monte Carlo samples", *Comput. Phys. Commun.* **77** (1993) 219, doi:10.1016/0010-4655(93)90005-W.

[59] CMS Collaboration, "Differential cross section measurements for the production of top quark pairs and of additional jets using dilepton events from pp collisions at $\sqrt{s} = 13$ TeV", *JHEP* **02** (2025) 064, doi:10.1007/JHEP02(2025)064, arXiv:2402.08486.

[60] J. Butterworth et al., "PDF4LHC recommendations for LHC Run II", *J. Phys. G* **43** (2016) 23001, doi:10.1088/0954-3899/43/2/023001, arXiv:1510.03865.

[61] G. Cowan, K. Cranmer, E. Gross, and O. Vitells, "Asymptotic formulae for likelihood-based tests of new physics", *Eur. Phys. J. C* **71** (2011) 1554, doi:10.1140/epjc/s10052-011-1554-0, arXiv:1007.1727. [Erratum: doi:10.1140/epjc/s10052-013-2501-z].

[62] S. Camarda et al., "DYTurbo: fast predictions for Drell–Yan processes", *Eur. Phys. J. C* **80** (2020) 251, doi:10.1140/epjc/s10052-020-7757-5, arXiv:1910.07049. [Erratum: doi:10.1140/epjc/s10052-020-7972-0].

[63] NNPDF Collaboration, "Nuclear parton distributions from lepton-nucleus scattering and the impact of an electron-ion collider", *Eur. Phys. J. C* **79** (2019) 471, doi:10.1140/epjc/s10052-019-6983-1, arXiv:1904.00018.

[64] R. Abdul Khalek et al., "nNNPDF3.0: evidence for a modified partonic structure in heavy nuclei", *Eur. Phys. J. C* **82** (2022) 507, doi:10.1140/epjc/s10052-022-10417-7, arXiv:2201.12363.

[65] I. Helenius, M. Walt, and W. Vogelsang, "NNLO nuclear parton distribution functions with electroweak-boson production data from the LHC", *Phys. Rev. D* **105** (2022) 094031, doi:10.1103/PhysRevD.105.094031, arXiv:2112.11904.

[66] NNPDF Collaboration, "Parton distributions for the LHC Run II", *JHEP* **04** (2015) 040, doi:10.1007/JHEP04(2015)040, arXiv:1410.8849.

A The CMS Collaboration

Yerevan Physics Institute, Yerevan, Armenia
A. Belyaev, A. Gevorgyan, A. Hayrapetyan, A. Tumasyan[1]

Marietta Blau Institute for Particle Physics, Vienna, Austria
W. Adam, L. Benato, T. Bergauer, M. Dragicevic, P.S. Hussain, M. Jeitler[2], N. Krammer, A. Li, D. Liko, M. Matthewman, J. Schieck[2], R. Schöfbeck[2], M. Shooshtari, M. Sonawane, N. Van Den Bossche, W. Waltenberger, C.-E. Wulz[2]

Universiteit Antwerpen, Antwerpen, Belgium
T. Janssen, H. Kwon, D. Ocampo Henao, T. Van Laer, P. Van Mechelen

Vrije Universiteit Brussel, Brussel, Belgium
D. Ahmadi, J. Bierkens, N. Breugelmans, J. D'Hondt, S. Dansana, A. De Moor, M. Delcourt, C. Gupta, F. Heyen, Y. Hong, P. Kashko, S. Lowette, I. Makarenko, S. Nandakumar, S. Tavernier, M. Tytgat[3], G.P. Van Onsem, S. Van Putte, D. Vannerom, T. Wybouw

Université Libre de Bruxelles, Bruxelles, Belgium
A. Beshr, B. Bilin, F. Caviglia Roman, B. Clerbaux, A.K. Das, I. De Bruyn, G. De Lentdecker, E. Ducarme, H. Evard, L. Favart, A. Khalilzadeh, A. Malara, M.A. Shahzad, A. Sharma, L. Thomas, M. Vanden Bemden, C. Vander Velde, P. Vanlaer, F. Zhang

Ghent University, Ghent, Belgium
A. Cauwels, M. De Coen, D. Dobur, C. Giordano, G. Gokbulut, K. Kaspar, D. Kavtaradze, D. Marckx, K. Skovpen, A.M. Tomaru, J. van der Linden, J. Vandenbroeck

Université Catholique de Louvain, Louvain-la-Neuve, Belgium
H. Aarup Petersen, A. Benecke, A. Bethani, G. Bruno, A. Cappati, J. De Favereau De Jeneret, C. Delaere, F. Gameiro Casalinho, A. Giammanco, A.O. Guzel, M. Hussain, V. Lemaitre, J. Lidrych, P. Malek, S. Turkcapar

Centro Brasileiro de Pesquisas Fisicas, Rio de Janeiro, Brazil
G.A. Alves, M. Barroso Ferreira Filho, E. Coelho, M.V. Gonçalves Sales, C. Hensel, D. Matos Figueiredo, T. Menezes De Oliveira, C. Mora Herrera, P. Rebello Teles, M. Soeiro, E.J. Tonelli Manganote[4], A. Vilela Pereira

Universidade do Estado do Rio de Janeiro, Rio de Janeiro, Brazil
W.L. Aldá Júnior, H. Brandao Malbouisson, W. Carvalho, J. Chinellato[5], M. Costa Reis, E.M. Da Costa, D. Da Silva Dalto, G.G. Da Silveira[6], D. De Jesus Damiao, S. Fonseca De Souza, R. Gomes De Souza, S. S. Jesus, T. Laux Kuhn[6], K. Maslova, K. Mota Amarilo, L. Mundim, H. Nogima, J.P. Pinheiro, A. Santoro, A. Sznajder, M. Thiel, F. Torres Da Silva De Araujo[7]

Universidade Estadual Paulista, Universidade Federal do ABC, São Paulo, Brazil
C.A. Bernardes, L. Calligaris, J. Carvalho Leite, F. Damas, T.R. Fernandez Perez Tomei, E.M. Gregores, B. Lopes Da Costa, I. Maietto Silverio, P.G. Mercadante, S.F. Novaes, Sandra S. Padula, V. Scheurer

Institute for Nuclear Research and Nuclear Energy, Bulgarian Academy of Sciences, Sofia, Bulgaria
A. Aleksandrov, G. Antchev, P. Danev, R. Hadjiiska, P. Iaydjiev, M. Shopova,

G. Sultanov

University of Sofia, Sofia, Bulgaria
A. Dimitrov, L. Litov, B. Pavlov, P. Petkov, A. Petrov

Instituto De Alta Investigación, Universidad de Tarapacá, Casilla 7 D, Arica, Chile
S. Keshri, D. Laroze, M. Meena, S. Thakur

Universidad Tecnica Federico Santa Maria, Valparaiso, Chile
W. Brooks

Beihang University, Beijing, China
T. Cheng, T. Javaid, L. Wang, L. Yuan

Department of Physics, Tsinghua University, Beijing, China
J. Gu, Z. Hu, Z. Liang, J. Liu, X. Wang, Y. Wang, H. Yang, S. Zhang

Institute of High Energy Physics, Beijing, China
N. Bi, G.M. Chen[8], H.S. Chen[8], M. Chen[8], Y. Chen, B. Hou, Q. Hou, F. Iemmi, C.H. Jiang, H. Liao, G. Liu, Z.-A. Liu[9], S. Song, J. Tao, C. Wang[8], J. Wang, A. Zada, H. Zhang, J. Zhao

State Key Laboratory of Nuclear Physics and Technology, Peking University, Beijing, China
A. Agapitos, Y. Ban, A. Carvalho Antunes De Oliveira, S. Deng, X. Geng, B. Guo, Q. Guo, Z. He, C. Jiang, A. Levin, C. Li, Q. Li, Y. Mao, S. Qian, S.J. Qian, X. Qin, C. Quaranta, X. Sun, D. Wang, J. Wang, T. Yang, M. Zhang, Y. Zhao, C. Zhou

State Key Laboratory of Nuclear Physics and Technology, Institute of Quantum Matter, South China Normal University, Guangzhou, China
X. Hua, S. Yang

Sun Yat-Sen University, Guangzhou, China
Z. You

University of Science and Technology of China, Hefei, China
N. Lu

Nanjing Normal University, Nanjing, China
G. Bauer[10,11], L. Chen, Z. Cui[11], B. Li[12], H. Wang, K. Yi[13], J. Zhang, F. Zhu

Institute of Frontier and Interdisciplinary Science, Shandong University, Qingdao, China
C. Li

Institute of Modern Physics and Key Laboratory of Nuclear Physics and Ion-beam Application (MOE) - Fudan University, Shanghai, China
Y. Li, Y. Zhou[14]

Zhejiang University, Hangzhou, Zhejiang, China
Z. Lin, C. Lu, M. Xiao[15]

Universidad de Los Andes, Bogota, Colombia
C. Avila, A. Cabrera, C. Florez, J.A. Reyes Vega

Universidad de Antioquia, Medellin, Colombia
C. Rendón, M. Rodriguez, A.A. Ruales Barbosa, J.D. Ruiz Alvarez

University of Split, Faculty of Electrical Engineering, Mechanical Engineering and Naval Architecture, Split, Croatia

N. Godinovic, D. Lelas, A. Sculac

University of Split, Faculty of Science, Split, Croatia
M. Kovac, A. Petkovic, T. Sculac

Institute Rudjer Boskovic, Zagreb, Croatia
P. Bargassa, V. Brigljevic, D. Ferencek, K. Jakovcic, A. Starodumov, T. Susa

University of Cyprus, Nicosia, Cyprus
A. Attikis, K. Christoforou, S. Konstantinou, C. Leonidou, L. Paizanos, F. Ptochos, P.A. Razis, H. Rykaczewski, H. Saka, A. Stepennov

Charles University, Prague, Czech Republic
M. Finger[†], M. Finger Jr.

Escuela Politecnica Nacional, Quito, Ecuador
E. Acurio

Universidad San Francisco de Quito, Quito, Ecuador
E. Carrera Jarrin

Academy of Scientific Research and Technology of the Arab Republic of Egypt, Egyptian Network of High Energy Physics, Cairo, Egypt
H. Abdalla[16], Y. Assran[17,18]

Center for High Energy Physics (CHEP-FU), Fayoum University, El-Fayoum, Egypt
A. Hussein, M.A. Mahmoud, H. Mohammed

National Institute of Chemical Physics and Biophysics, Tallinn, Estonia
K. Jaffel, M. Kadastik, T. Lange, C. Nielsen, J. Pata, M. Raidal, N. Seeba, L. Tani

Department of Physics, University of Helsinki, Helsinki, Finland
E. Brücken, A. Milieva, K. Osterberg, M. Voutilainen

Helsinki Institute of Physics, Helsinki, Finland
F. Garcia, T. Hilden, P. Inkaew, K.T.S. Kallonen, R. Kumar Verma, T. Lampén, K. Lassila-Perini, B. Lehtela, S. Lehti, T. Lindén, N.R. Mancilla Xinto, M. Myllymäki, M.m. Rantanen, S. Saariokari, N.T. Toikka, J. Tuominiemi

Lappeenranta-Lahti University of Technology, Lappeenranta, Finland
N. Bin Norjoharuddeen, H. Kirschenmann, P. Luukka, H. Petrow

IRFU, CEA, Université Paris-Saclay, Gif-sur-Yvette, France
M. Besancon, F. Couderc, M. Dejardin, D. Denegri, P. Devouge, J.L. Faure, F. Ferri, P. Gaigne, S. Ganjour, P. Gras, F. Guilloux, G. Hamel de Monchenault, M. Kumar, V. Lohezic, Y. Maidannyk, J. Malcles, F. Orlandi, L. Portales, S. Ronchi, M.Ö. Sahin, P. Simkina, M. Titov, M. Tornago

Laboratoire Leprince-Ringuet, CNRS/IN2P3, Ecole Polytechnique, Institut Polytechnique de Paris, Palaiseau, France
R. Amella Ranz, F. Beaudette, G. Boldrini, P. Busson, C. Charlot, M. Chiusi, T.D. Cuisset, O. Davignon, A. De Wit, T. Debnath, I.T. Ehle, S. Ghosh, A. Gilbert, R. Granier de Cassagnac, M. Manoni, M. Nguyen, S. Obraztsov, C. Ochando, R. Salerno, J.B. Sauvan, Y. Sirois, G. Sokmen, Y. Song, L. Urda Gómez, B. Voirin, A. Zabi, A. Zghiche

Université de Strasbourg, CNRS, IPHC UMR 7178, Strasbourg, France

J.-L. Agram[19], J. Andrea, D. Bloch, J.-M. Brom, E.C. Chabert, C. Collard, G. Coulon, S. Falke, U. Goerlach, A.-C. Le Bihan, G. Saha, A. Savoy-Navarro[20], P. Vaucelle

Centre de Calcul de l'Institut National de Physique Nucleaire et de Physique des Particules, CNRS/IN2P3, Villeurbanne, France
A. Di Florio, B. Orzari

Institut de Physique des 2 Infinis de Lyon (IP2I), Villeurbanne, France
D. Amram, S. Beauceron, B. Blancon, G. Boudoul, N. Chanon, D. Contardo, P. Depasse, H. El Mamouni, J. Fay, E. Fillaudeau, S. Gascon, M. Gouzevitch, C. Greenberg, G. Grenier, B. Ille, E. Jourd'Huy, M. Lethuillier, K. Long, B. Massoteau, L. Mirabito, A. Purohit, M. Vander Donckt, C. Verollet

Georgian Technical University, Tbilisi, Georgia
A. Khvedelidze[21], I. Lomidze, Z. Tsamalaidze[21]

RWTH Aachen University, I. Physikalisches Institut, Aachen, Germany
K.F. Adamowicz, V. Botta, S. Consuegra Rodríguez, L. Feld, K. Klein, M. Lipinski, P. Nattland, V. Oppenländer, A. Pauls, D. Pérez Adán

RWTH Aachen University, III. Physikalisches Institut A, Aachen, Germany
C. Daumann, S. Diekmann, N. Eich, D. Eliseev, F. Engelke, J. Erdmann, M. Erdmann, M.Z. Farkas, B. Fischer, T. Hebbeker, K. Hoepfner, A. Jung, N. Kumar, M.y. Lee, F. Mausolf, M. Merschmeyer, A. Meyer, A. Pozdnyakov, W. Redjeb, H. Reithler, U. Sarkar, V. Sarkisovi, A. Schmidt, C. Seth, A. Sharma, J.L. Spah, V. Vaulin, U. Willemsen, S. Zaleski, F.P. Zinn

RWTH Aachen University, III. Physikalisches Institut B, Aachen, Germany
M.R. Beckers, G. Flügge, N. Hoeflich, T. Kress, A. Nowack, O. Pooth, A. Stahl

Deutsches Elektronen-Synchrotron, Hamburg, Germany
A. Abel, M. Aldaya Martin, J. Alimena, Y. An, I. Andreev, J. Bach, S. Baxter, H. Becerril Gonzalez, O. Behnke, A. Belvedere, F. Blekman[22], K. Borras[23], A. Campbell, S. Chatterjee, L.X. Coll Saravia, G. Eckerlin, D. Eckstein, E. Gallo[22], A. Geiser, M. Guthoff, A. Hinzmann, M. Kasemann, C. Kleinwort, R. Kogler, M. Komm, D. Krücker, F. Labe, W. Lange, D. Leyva Pernia, J.h. Li, K.-Y. Lin, K. Lipka[24], W. Lohmann[25], J. Malvaso, R. Mankel, I.-A. Melzer-Pellmann, M. Mendizabal Morentin, A.B. Meyer, G. Milella, K. Moral Figueroa, A. Mussgiller, L.P. Nair, J. Niedziela, A. Nürnberg, J. Park, E. Ranken, A. Raspereza, D. Rastorguev, L. Rygaard, M. Scham[26,23], S. Schnake[23], P. Schütze, C. Schwanenberger[22], D. Schwarz, D. Selivanova, K. Sharko, M. Shchedrolosiev, D. Stafford, M. Torkian, S. Vashishtha, A. Ventura Barroso, R. Walsh, D. Wang, Q. Wang, K. Wichmann, L. Wiens[23], C. Wissing, Y. Yang, S. Zakharov, A. Zimermmane Castro Santos

University of Hamburg, Hamburg, Germany
A.R. Alves Andrade, M. Antonello, S. Bollweg, M. Bonanomi, L. Ebeling, K. El Morabit, Y. Fischer, M. Frahm, E. Garutti, A. Grohsjean, A.A. Guvenli, J. Haller, D. Hundhausen, M. Jalalvandi, G. Kasieczka, P. Keicher, R. Klanner, W. Korcari, T. Kramer, C.c. Kuo, J. Lange, A. Lobanov, J. Matthiesen, L. Moureaux, K. Nikolopoulos, K.J. Pena Rodriguez, N. Prouvost, B. Raciti, M. Rieger, D. Savoiu, P. Schleper, M. Schröder, J. Schwandt, T. Tore von Schwartz, M. Sommerhalder,

H. Stadie, G. Steinbrück, R. Ward, B. Wiederspan, M. Wolf, C. Yede

Karlsruher Institut fuer Technologie, Karlsruhe, Germany
A. Brusamolino, E. Butz, Y.M. Chen, T. Chwalek, A. Dierlamm, G.G. Dincer, D. Druzhkin, U. Elicabuk, N. Faltermann, M. Giffels, A. Gottmann, F. Hartmann[27], F. Hummer, U. Husemann, J. Kieseler, M. Klute, J. Knolle, R. Kunnilan Muhammed Rafeek, O. Lavoryk, J.M. Lawhorn, S. Maier, T. Mehner, M. Molch, A.A. Monsch, M. Mormile, Th. Müller, E. Pfeffer, M. Presilla, G. Quast, K. Rabbertz, B. Regnery, R. Schmieder, T. Selezneva, N. Shadskiy, I. Shvetsov, H.J. Simonis, L. Sowa, L. Stockmeier, K. Tauqeer, M. Toms, B. Topko, N. Trevisani, C. Verstege, T. Voigtländer, R.F. Von Cube, J. Von Den Driesch, C. Winter, R. Wolf, W.D. Zeuner, X. Zuo

Institute of Nuclear and Particle Physics (INPP), NCSR Demokritos, Aghia Paraskevi, Greece
G. Anagnostou, G. Daskalakis, A. Kyriakis

National and Kapodistrian University of Athens, Athens, Greece
P. Iosifidou, P. Katris, G. Melachroinos, Z. Painesis, I. Paraskevas, N. Plastiras, N. Saoulidou, K. Theofilatos, E. Tziaferi, E. Tzovara, K. Vellidis, I. Zisopoulos

National Technical University of Athens, Athens, Greece
T. Chatzistavrou, G. Karapostoli, K. Kousouris, K. Paschos, E. Siamarkou, G. Tsipolitis

University of Ioánnina, Ioánnina, Greece
I. Evangelou, C. Foudas, P. Katsoulis, P. Kokkas, P.G. Kosmoglou Kioseoglou, N. Manthos, I. Papadopoulos, J. Strologas

HUN-REN Wigner Research Centre for Physics, Budapest, Hungary
C. Hajdu, D. Horvath[28,29], Á. Kadlecsik, C. Lee, K. Márton, A.J. Rádl[30], F. Sikler, V. Veszpremi

MTA-ELTE Lendület CMS Particle and Nuclear Physics Group, Eötvös Loránd University, Budapest, Hungary
G. Balint, D. Biro, M. Csanád, K. Farkas, A. Fehérkuti[31], M.M.A. Gadallah[32], M. León Coello, G. Pásztor, G.I. Veres

Faculty of Informatics, University of Debrecen, Debrecen, Hungary
B. Ujvari, G. Zilizi

HUN-REN ATOMKI - Institute of Nuclear Research, Debrecen, Hungary
G. Bencze, S. Czellar, J. Molnar, Z. Szillasi

Karoly Robert Campus, MATE Institute of Technology, Gyongyos, Hungary
T. Csorgo[31], F. Nemes[31], T. Novak, I. Szanyi[33]

IIT Bhubaneswar, Bhubaneswar, India
S. Bahinipati, R. Raturi

Panjab University, Chandigarh, India
S. Bansal, S.B. Beri, V. Bhatnagar, B. Chauhan, S. Chauhan, N. Dhingra[34], A. Kaur, H. Kaur, M. Kaur, S. Kumar, T. Sheokand, J.B. Singh, A. Singla, K. Verma

University of Delhi, Delhi, India
A. Bhardwaj, A. Chhetri, B.C. Choudhary, A. Kumar, A. Kumar, M. Naimuddin,

S. Phor, C. Prakash, K. Ranjan, M.K. Saini

Indian Institute of Technology Mandi (IIT-Mandi), Himachal Pradesh, India
M. Kumari, P. Palni, S. Rana, A. Rathore

University of Hyderabad, Hyderabad, India
S. Acharya[35], B. Gomber

Indian Institute of Technology Kanpur, Kanpur, India
S. Ganguly, S. Mukherjee

Saha Institute of Nuclear Physics, HBNI, Kolkata, India
S. Bhattacharya, S. Das Gupta, S. Dutta, S. Dutta, S. Sarkar

Indian Institute of Technology Madras, Madras, India
M.M. Ameen, P.K. Behera, S. Chatterjee, G. Dash, A. Dattamunsi, P. Jana, P. Kalbhor, S. Kamble, J.R. Komaragiri[36], P.R. Pujahari, A.K. Sikdar, R.K. Singh, P. Verma, S. Verma, A. Vijay

IISER Mohali, India, Mohali, India
S. Nayak, H. Rajpoot, B.K. Sirasva

Tata Institute of Fundamental Research-A, Mumbai, India
L. Bhatt, S. Dugad, T. Mishra, G.B. Mohanty, M. Shelake, P. Suryadevara

Tata Institute of Fundamental Research-B, Mumbai, India
A. Bala, S. Banerjee, S. Barman[37], R.M. Chatterjee, J. Chhikara, M. Guchait, Sh. Jain, A. Jaiswal, S. Kumar, M. Maity[37], G. Majumder, K. Mazumdar, S. Parolia, R. Pramanik, R. Saxena, A. Thachayath

National Institute of Science Education and Research, An OCC of Homi Bhabha National Institute, Bhubaneswar, Odisha, India
D. Maity[38], P. Mal, K. Naskar[38], A. Nayak[38], K. Pal, P. Sadangi, S. Shuchi, S.K. Swain, S. Varghese[38], D. Vats[38]

Indian Institute of Science Education and Research (IISER), Pune, India
S. Dube, P. Hazarika, B. Kansal, A. Laha, R. Sharma, S. Sharma, K.Y. Vaish

Indian Institute of Technology Hyderabad, Telangana, India
B. Babu, S. Ghosh

Isfahan University of Technology, Isfahan, Iran
H. Bakhshiansohi[39], A. Jafari[40], V. Sedighzadeh Dalavi, M. Zeinali[41]

Institute for Research in Fundamental Sciences (IPM), Tehran, Iran
S. Bashiri, S. Chenarani[42], S.M. Etesami, Y. Hosseini, M. Khakzad, E. Khazaie, M. Mohammadi Najafabadi, M. Nourbakhsh, S. Tizchang[43]

University College Dublin, Dublin, Ireland
M. Felcini, M. Grunewald

INFN Sezione di Bari[a], Università di Bari[b], Politecnico di Bari[c], Bari, Italy
M. Abbrescia[a,b], M. Barbieri[a,b], M. Buonsante[a,b], A. Colaleo[a,b], D. Creanza[a,c], N. De Filippis[a,c], M. De Palma[a,b], W. Elmetenawee[a,b,44], N. Ferrara[a,c], L. Fiore[a], L. Generoso[a,b], L. Longo[a], M. Louka[a,b], G. Maggi[a,c], M. Maggi[a], I. Margjeka[a], V. Mastrapasqua[a,b], S. My[a,b], F. Nenna[a,b], S. Nuzzo[a,b], A. Pellecchia[a,b], A. Pompili[a,b], F.M. Procacci[a,b], G. Pugliese[a,c], R. Radogna[a,b], D. Ramos[a],

A. Ranieri[a], L. Silvestris[a], F.M. Simone[a,c], Ü. Sözbilir[a], A. Stamerra[a,b], D. Troiano[a,b], R. Venditti[a,b], P. Verwilligen[a], A. Zaza[a,b]

INFN Sezione di Bologna[a], Università di Bologna[b], Bologna, Italy
C. Battilana[a,b], D. Bonacorsi[a,b], P. Capiluppi[a,b], F.R. Cavallo[a], M. Cruciani[a,b], M. Cuffiani[a,b], G.M. Dallavalle[a], T. Diotalevi[a,b], F. Fabbri[a], A. Fanfani[a,b], R. Farinelli[a], D. Fasanella[a], L. Ferragina[a,b], P. Giacomelli[a], L. Guiducci[a,b], S. Lo Meo[a,45], M. Lorusso[a,b], L. Lunerti[a], S. Marcellini[a], G. Masetti[a], F.L. Navarria[a,b], G. Paggi[a,b], A. Perrotta[a], A.M. Rossi[a,b], S. Rossi Tisbeni[a,b], T. Rovelli[a,b], G.P. Siroli[a,b]

INFN Sezione di Catania[a], Università di Catania[b], Catania, Italy
S. Costa[a,b,46], A. Di Mattia[a], A. Lapertosa[a], R. Potenza[a,b], A. Tricomi[a,b,46]

INFN Sezione di Firenze[a], Università di Firenze[b], Firenze, Italy
J. Altork[a,b], P. Assiouras[a], G. Barbagli[a], G. Bardelli[a], M. Bartolini[a,b], A. Calandri[a,b], B. Camaiani[a,b], A. Cassese[a], R. Ceccarelli[a], V. Ciulli[a,b], C. Civinini[a], R. D'Alessandro[a,b], L. Damenti[a,b], E. Focardi[a,b], T. Kello[a], G. Latino[a,b], P. Lenzi[a,b], M. Lizzo[a], M. Meschini[a], S. Paoletti[a], A. Papanastassiou[a,b], G. Sguazzoni[a], L. Viliani[a]

INFN Laboratori Nazionali di Frascati, Frascati, Italy
L. Benussi, S. Colafranceschi[47], S. Meola[48], D. Piccolo

INFN Sezione di Genova[a], Università di Genova[b], Genova, Italy
M. Alves Gallo Pereira[a], F. Ferro[a], E. Robutti[a], S. Tosi[a,b]

INFN Sezione di Milano-Bicocca[a], Università di Milano-Bicocca[b], Milano, Italy
A. Benaglia[a], F. Brivio[a], V. Camagni[a,b], F. Cetorelli[a,b], F. De Guio[a,b], M.E. Dinardo[a,b], P. Dini[a], S. Gennai[a], R. Gerosa[a,b], A. Ghezzi[a,b], P. Govoni[a,b], L. Guzzi[a], M.R. Kim[a], G. Lavizzari[a,b], M.T. Lucchini[a,b], M. Malberti[a], S. Malvezzi[a], A. Massironi[a], D. Menasce[a], L. Moroni[a], M. Paganoni[a,b], S. Palluotto[a,b], D. Pedrini[a], A. Perego[a,b], T. Tabarelli de Fatis[a,b]

INFN Sezione di Napoli[a], Università di Napoli 'Federico II'[b], Napoli, Italy; Università della Basilicata[c], Potenza, Italy; Scuola Superiore Meridionale (SSM)[d], Napoli, Italy
S. Buontempo[a], F. Confortini[a,b], C. Di Fraia[a,b], F. Fabozzi[a,c], L. Favilla[a,d], A.O.M. Iorio[a,b], L. Lista[a,b,49], P. Paolucci[a,27], B. Rossi[a]

INFN Sezione di Padova[a], Università di Padova[b], Padova, Italy; Universita degli Studi di Cagliari[c], Cagliari, Italy
P. Azzi[a], N. Bacchetta[a,50], D. Bisello[a,b], L. Borella[a], P. Bortignon[a,c], G. Bortolato[a,b], A.C.M. Bulla[a,c], R. Carlin[a,b], P. Checchia[a], T. Dorigo[a,51], F. Gasparini[a,b], S. Giorgetti[a], F. Gonella[a], P. Grutta[a], N. Lai[a], E. Lusiani[a], M. Margoni[a,b], A.T. Meneguzzo[a,b], M. Missiroli[a], J. Pazzini[a,b], F. Primavera[a,b], P. Ronchese[a,b], R. Rossin[a,b], M. Tosi[a,b], A. Triossi[a,b], S. Ventura[a], M. Zanetti[a,b], P. Zotto[a,b], A. Zucchetta[a,b], G. Zumerle[a,b]

INFN Sezione di Pavia[a], Università di Pavia[b], Pavia, Italy
C. Aimè[a], A. Braghieri[a], M. Brunoldi[a,b], S. Calzaferri[a,b], P. Montagna[a,b], M. Pelliccioni[a,b], V. Re[a], C. Riccardi[a,b], P. Salvini[a], I. Vai[a,b], P. Vitulo[a,b]

INFN Sezione di Perugia[a], Università di Perugia[b], Perugia, Italy
S. Ajmal[a,b], M.E. Ascioti[a,b], G.M. Bilei[†a], C. Carrivale[a,b], D. Ciangottini[a,b],

L. Della Penna[a,b], L. Fanò[a,b], V. Mariani[a,b], M. Menichelli[a], F. Moscatelli[a,52], A. Rossi[a,b], A. Santocchia[a,b], D. Spiga[a], T. Tedeschi[a,b]

INFN Sezione di Pisa[a], Università di Pisa[b], Scuola Normale Superiore di Pisa[c], Pisa, Italy; Università di Siena[d], Siena, Italy
C.A. Alexe[a,c], P. Asenov[a,b], P. Azzurri[a], G. Bagliesi[a], L. Bianchini[a,b], T. Boccali[a], E. Bossini[a], D. Bruschini[a,c], R. Castaldi[a], F. Cattafesta[a,c], M.A. Ciocci[a,d], M. Cipriani[a,b], R. Dell'Orso[a], S. Donato[a,b], A. Feliziani[a,d], R. Forti[a,b], A. Giassi[a], F. Ligabue[a,c], A.C. Marini[a,b], A. Messineo[a,b], S. Mishra[a], V.K. Muraleedharan Nair Bindhu[a,b], S. Nandan[a], F. Palla[a], M. Riggirello[a,c], A. Rizzi[a,b], G. Rolandi[a,c], S. Roy Chowdhury[a,53], T. Sarkar[a], A. Scribano[a], P. Solanki[a,b], P. Spagnolo[a], F. Tenchini[a,b], R. Tenchini[a], G. Tonelli[a,b], N. Turini[a,d], F. Vaselli[a,c], A. Venturi[a], P.G. Verdini[a]

INFN Sezione di Roma[a], Sapienza Università di Roma[b], Roma, Italy
P. Akrap[a,b], C. Basile[a,b], S.C. Behera[a], F. Cavallari[a], L. Cunqueiro Mendez[a,b], F. De Riggi[a,b], D. Del Re[a,b], M. Del Vecchio[a,b], E. Di Marco[a], M. Diemoz[a], F. Errico[a], L. Frosina[a,b], R. Gargiulo[a,b], B. Harikrishnan[a,b], F. Lombardi[a,b], E. Longo[a,b], L. Martikainen[a,b], G. Organtini[a,b], N. Palmeri[a,b], R. Paramatti[a,b], T. Pauletto[a,b], S. Rahatlou[a,b], C. Rovelli[a], F. Santanastasio[a,b], L. Soffi[a], V. Vladimirov[a,b]

INFN Sezione di Torino[a], Università di Torino[b], Torino, Italy; Università del Piemonte Orientale[c], Novara, Italy
N. Amapane[a,b], R. Arcidiacono[a,c], S. Argiro[a,b], M. Arneodo[†a,c], N. Bartosik[a,c], R. Bellan[a,b], A. Bellora[a,b], C. Biino[a], C. Borca[a,b], N. Cartiglia[a], M. Costa[a,b], R. Covarelli[a,b], N. Demaria[a], E. Ferrando[a,b], L. Finco[a], M. Grippo[a,b], B. Kiani[a,b], L. Lanteri[a,b], F. Legger[a], F. Luongo[a,b], M. Marchisio Caprioglio[a,b], C. Mariotti[a], S. Maselli[a], A. Mecca[a,b], L. Menzio[a,b], P. Meridiani[a], E. Migliore[a,b], M. Monteno[a], M.M. Obertino[a,b], G. Ortona[a], L. Pacher[a,b], N. Pastrone[a], M. Ruspa[a,c], F. Siviero[a,b], V. Sola[a,b], A. Solano[a,b], A. Staiano[a], C. Tarricone[a,b], D. Trocino[a], G. Umoret[a,b], E. Vlasov[a,b], R. White[a,b]

INFN Sezione di Trieste[a], Università di Trieste[b], Trieste, Italy
J. Babbar[a,b,53], S. Belforte[a], V. Candelise[a,b], M. Casarsa[a], F. Cossutti[a], K. De Leo[a], G. Della Ricca[a,b], R. Delli Gatti[a,b], C. Giraldin[a,b]

Kyungpook National University, Daegu, Korea
S. Dogra, J. Hong, J. Kim, T. Kim, D. Lee, H. Lee, J. Lee, S.W. Lee, C.S. Moon, Y.D. Oh, S. Sekmen, B. Tae, Y.C. Yang

Department of Mathematics and Physics - GWNU, Gangneung, Korea
M.S. Kim

Chonnam National University, Institute for Universe and Elementary Particles, Kwangju, Korea
G. Bak, P. Gwak, H. Kim, H. Lee, S. Lee, D.H. Moon, J. Seo

Hanyang University, Seoul, Korea
E. Asilar, F. Carnevali, J. Choi[54], T.J. Kim, Y. Ryou, J. Song

Korea University, Seoul, Korea
S. Ha, S. Han, B. Hong, J. Kim, K. Lee, K.S. Lee, S. Lee, J. Padmanaban, J. Yoo

Kyung Hee University, Department of Physics, Seoul, Korea
J. Goh, J. Shin, S. Yang

Sejong University, Seoul, Korea
L. Kalipoliti, Y. Kang, H. S. Kim, Y. Kim, B. Ko, S. Lee

Seoul National University, Seoul, Korea
J. Almond, J.H. Bhyun, J. Choi, J. Choi, W. Jun, H. Kim, J. Kim, J. Kim, T. Kim, Y. Kim, Y.W. Kim, S. Ko, H. Lee, J. Lee, J. Lee, B.H. Oh, J. Shin, U.K. Yang, I. Yoon

University of Seoul, Seoul, Korea
W. Heo, W. Jang, D. Kim, S. Kim, J.S.H. Lee, Y. Lee, I.C. Park, Y. Roh, I.J. Watson

Yonsei University, Department of Physics, Seoul, Korea
G. Cho, Y. Eo, K. Hwang, H. Jang, B. Kim, D. Kim, S. Kim, K. Lee, G. Mocellin, H.D. Yoo

Sungkyunkwan University, Suwon, Korea
Y. Lee, I. Yu

College of Engineering and Technology, American University of the Middle East (AUM), Dasman, Kuwait
T. Beyrouthy, Y. Gharbia

Kuwait University - College of Science - Department of Physics, Safat, Kuwait
F. Alazemi

Riga Technical University, Riga, Latvia
K. Dreimanis, O.M. Eberlins, A. Gaile, M. Klevs, C. Munoz Diaz, D. Osite, G. Pikurs, R. Plese, A. Potrebko, M. Seidel, D. Sidiropoulos Kontos

University of Latvia (LU), Riga, Latvia
N.R. Strautnieks

Vilnius University, Vilnius, Lithuania
M. Ambrozas, A. Juodagalvis, S. Nargelas, S. Nayak, A. Rinkevicius, G. Tamulaitis

National Centre for Particle Physics, Universiti Malaya, Kuala Lumpur, Malaysia
I. Yusuff[55], Z. Zolkapli

Universidad de Sonora (UNISON), Hermosillo, Mexico
J.F. Benitez, A. Castaneda Hernandez, A. Cota Rodriguez, L.E. Cuevas Picos, H.A. Encinas Acosta, L.G. Gallegos Maríñez, J.A. Murillo Quijada, L. Valencia Palomo

Centro de Investigacion y de Estudios Avanzados del IPN, Mexico City, Mexico
G. Ayala, H. Castilla-Valdez, H. Crotte Ledesma, R. Lopez-Fernandez, J. Mejia Guisao, R. Reyes-Almanza, A. Sánchez Hernández

Universidad Iberoamericana, Mexico City, Mexico
C. Oropeza Barrera, D.L. Ramirez Guadarrama, M. Ramírez García

Benemerita Universidad Autonoma de Puebla, Puebla, Mexico
I. Bautista, F.E. Neri Huerta, I. Pedraza, H.A. Salazar Ibarguen, C. Uribe Estrada

University of Montenegro, Podgorica, Montenegro
I. Bubanja, J. Mijuskovic, N. Raicevic

University of Canterbury, Christchurch, New Zealand
P.H. Butler

National Centre for Physics, Quaid-I-Azam University, Islamabad, Pakistan
A. Ahmad, M.I. Asghar, A. Awais, M.I.M. Awan, W.A. Khan

AGH University of Krakow, Krakow, Poland
V. Avati, L. Forthomme, L. Grzanka, M. Malawski, K. Piotrzkowski

National Centre for Nuclear Research, Swierk, Poland
H. Awedikian, M. Bluj, M. Ghimiray, M. Górski, M. Kazana, M. Szleper, P. Zalewski

Institute of Experimental Physics, Faculty of Physics, University of Warsaw, Warsaw, Poland
K. Bunkowski, K. Doroba, A. Kalinowski, M. Konecki, J. Krolikowski, W. Matyszkiewicz, A. Muhammad, S. Slawinski

Warsaw University of Technology, Warsaw, Poland
P. Fokow, K. Pozniak, W. Zabolotny

Laboratório de Instrumentação e Física Experimental de Partículas, Lisboa, Portugal
M. Araujo, C. Beirão Da Cruz E Silva, A. Boletti, M. Bozzo, T. Camporesi, G. Da Molin, M. Gallinaro, J. Hollar, N. Leonardo, G.B. Marozzo, A. Petrilli, M. Pisano, J. Seixas, J. Varela, J.W. Wulff

Faculty of Physics, University of Belgrade, Belgrade, Serbia
P. Adzic, L. Markovic, P. Milenovic, V. Milosevic

VINCA Institute of Nuclear Sciences, University of Belgrade, Belgrade, Serbia
D. Devetak, M. Dordevic, J. Milosevic, L. Nadderd, V. Rekovic, M. Stojanovic

Centro de Investigaciones Energéticas Medioambientales y Tecnológicas (CIEMAT), Madrid, Spain
M. Alcalde Martinez, J. Alcaraz Maestre, Cristina F. Bedoya, J.A. Brochero Cifuentes, Oliver M. Carretero, M. Cepeda, M. Cerrada, N. Colino, B. De La Cruz, A. Delgado Peris, A. Escalante Del Valle, D. Fernández Del Val, J.P. Fernández Ramos, J. Flix, M.C. Fouz, M. Gonzalez Hernandez, O. Gonzalez Lopez, S. Goy Lopez, J.M. Hernandez, M.I. Josa, J. Llorente Merino, C. Martin Perez, E. Martin Viscasillas, D. Moran, C. M. Morcillo Perez, Á. Navarro Tobar, R. Paz Herrera, A. Pérez-Calero Yzquierdo, J. Puerta Pelayo, I. Redondo, J. Vazquez Escobar

Universidad Autónoma de Madrid, Madrid, Spain
J.F. de Trocóniz

Universidad de Oviedo, Instituto Universitario de Ciencias y Tecnologías Espaciales de Asturias (ICTEA), Oviedo, Spain
E. Aller Gutierrez, B. Alvarez Gonzalez, J. Ayllon Torresano, A. Cardini, J. Cuevas, J. Del Riego Badas, D. Estrada Acevedo, J. Fernandez Menendez, S. Folgueras, I. Gonzalez Caballero, P. Leguina, M. Obeso Menendez, E. Palencia Cortezon, J. Prado Pico, S. Sanchez Cruz, A. Soto Rodríguez, P. Vischia

Instituto de Física de Cantabria (IFCA), CSIC-Universidad de Cantabria, Santander, Spain
S. Blanco Fernández, I.J. Cabrillo, A. Calderon, M. Caserta, J. Duarte Campderros,

M. Fernandez, G. Gomez, C. Lasaosa García, R. Lopez Ruiz, C. Martinez Rivero, P. Martinez Ruiz del Arbol, F. Matorras, P. Matorras Cuevas, E. Navarrete Ramos, J. Piedra Gomez, C. Quintana San Emeterio, V. Rodriguez, L. Scodellaro, I. Vila, R. Vilar Cortabitarte, J.M. Vizan Garcia

University of Colombo, Colombo, Sri Lanka
B. Kailasapathy[56], D.D.C. Wickramarathna

University of Ruhuna, Department of Physics, Matara, Sri Lanka
W.G.D. Dharmaratna[57], K. Liyanage, N. Perera

CERN, European Organization for Nuclear Research, Geneva, Switzerland
D. Abbaneo, C. Amendola, R. Ardino, E. Auffray, J. Baechler, D. Barney, J. Bendavid, I. Bestintzanos, M. Bianco, A. Bocci, L. Borgonovi, C. Botta, A. Bragagnolo, C.E. Brown, C. Caillol, G. Cerminara, P. Connor, K. Cormier, D. d'Enterria, A. Dabrowski, P. Das, A. David, A. De Roeck, M.M. Defranchis, M. Deile, M. Dobson, P.J. Fernández Manteca, B.A. Fontana Santos Alves, E. Fontanesi, W. Funk, A. Gaddi, S. Giani, D. Gigi, K. Gill, F. Glege, M. Glowacki, A. Gruber, J. Hegeman, J.K. Heikkilä, R. Hofsaess, B. Huber, T. James, P. Janot, L. Jeppe, O. Kaluzinska, O. Karacheban[25], G. Karathanasis, S. Laurila, P. Lecoq, J. León Holgado, E. Leutgeb, C. Lourenço, A.-M. Lyon, M. Magherini, L. Malgeri, M. Mannelli, A. Mehta, F. Meijers, J.A. Merlin, S. Mersi, E. Meschi, M. Migliorini, F. Monti, F. Moortgat, M. Mulders, M. Musich, I. Neutelings, S. Orfanelli, F. Pantaleo, M. Pari, F. Pereira Carneiro, G. Petrucciani, A. Pfeiffer, M. Pierini, M. Pitt, H. Qu, D. Rabady, A. Reimers, B. Ribeiro Lopes, F. Riti, P. Rosado, M. Rovere, H. Sakulin, R. Salvatico, S. Scarfi, S.F. Schaefer, M. Selvaggi, K. Shchelina, P. Silva, P. Sphicas[58], A.G. Stahl Leiton, A. Steen, S. Summers, G. Terragni, D. Treille, P. Tropea, E. Vernazza, M. Vojinovic, J. Wanczyk[59], S. Wuchterl, M. Zarucki, P. Zehetner, P. Zejdl, G. Zevi Della Porta

PSI Center for Neutron and Muon Sciences, Villigen, Switzerland
L. Caminada[60], W. Erdmann, R. Horisberger, Q. Ingram, H.C. Kaestli, D. Kotlinski, C. Lange, U. Langenegger, A. Nigamova, L. Noehte[60], L. Redard-Jacot[60], T. Rohe, A. Samalan

ETH Zurich - Institute for Particle Physics and Astrophysics (IPA), Zurich, Switzerland
T.K. Aarrestad, M. Backhaus, T. Bevilacqua[60], G. Bonomelli, C. Cazzaniga, K. Datta, P. De Bryas Dexmiers D'Archiacchiac[59], A. De Cosa, G. Dissertori, M. Dittmar, M. Donegà, F. Glessgen, C. Grab, N. Härringer, T.G. Harte, M.Köppel, W. Lustermann, M. Malucchi, R.A. Manzoni, L. Marchese, A. Mascellani[59], F. Nessi-Tedaldi, F. Pauss, A.A. Petre, J. Prendi, B. Ristic, S. Rohletter, P.M. Sander, R. Seidita, J. Steggemann[59], A. Tarabini, C.Z. Tee, D. Valsecchi, P.H. Wagner, R. Wallny

Universität Zürich, Zurich, Switzerland
C. Amsler[61], P. Bärtschi, F. Bilandzija, M.F. Canelli, G. Celotto, T.A. Goldschmidt, V. Guglielmi, A. Jofrehei, B. Kilminster, T.H. Kwok, S. Leontsinis, V. Lukashenko, A. Macchiolo, F. Meng, J. Motta, P. Robmann, E. Shokr, F. Stäger, R. Tramontano, P. Viscone

National Central University, Chung-Li, Taiwan
D. Bhowmik, C.M. Kuo, P.K. Rout, S. Taj, P.C. Tiwari[36]

National Taiwan University (NTU), Taipei, Taiwan
L. Ceard, K.F. Chen, Z.g. Chen, A. De Iorio, W.-S. Hou, T.h. Hsu, Y.w. Kao, S. Karmakar, F. Khuzaimah, G. Kole, Y.y. Li, R.-S. Lu, E. Paganis, X.f. Su, J. Thomas-Wilsker, L.s. Tsai, D. Tsionou, H.y. Wu, E. Yazgan

High Energy Physics Research Unit, Department of Physics, Faculty of Science, Chulalongkorn University, Bangkok, Thailand
C. Asawatangtrakuldee, N. Srimanobhas

Tunis El Manar University, Tunis, Tunisia
Y. Maghrbi

Çukurova University, Physics Department, Science and Art Faculty, Adana, Turkey
D. Agyel, F. Dolek, I. Dumanoglu[62], Y. Guler[63], E. Gurpinar Guler[63], O. Kara[64], A. Kayis Topaksu, Y. Komurcu, G. Onengut, K. Ozdemir[65], B. Tali[66], U.G. Tok, E. Uslan, I.S. Zorbakir

Hacettepe University, Ankara, Turkey
S. Sen

Middle East Technical University, Physics Department, Ankara, Turkey
M. Yalvac[67]

Bogazici University, Istanbul, Turkey
B. Akgun, I.O. Atakisi[68], E. Gülmez, M. Kaya[69], O. Kaya[70], M.A. Sarkisla[71], S. Tekten[72]

Istanbul Technical University, Istanbul, Turkey
D. Boncukcu, A. Cakir, K. Cankocak[62,73]

Istanbul University, Istanbul, Turkey
B. Hacisahinoglu, I. Hos[74], B. Kaynak, S. Ozkorucuklu, O. Potok, H. Sert, C. Simsek, C. Zorbilmez

Yildiz Technical University, Istanbul, Turkey
S. Cerci, C. Dozen[75], B. Isildak, E. Simsek, D. Sunar Cerci, T. Yetkin[75]

Institute for Scintillation Materials of National Academy of Science of Ukraine, Kharkiv, Ukraine
A. Boyaryntsev, O. Dadazhanova, B. Grynyov

National Science Centre, Kharkiv Institute of Physics and Technology, Kharkiv, Ukraine
L. Levchuk

University of Bristol, Bristol, United Kingdom
J.J. Brooke, A. Bundock, F. Bury, E. Clement, D. Cussans, D. Dharmender, H. Flacher, J. Goldstein, H.F. Heath, M.-L. Holmberg, A. Karakoulaki, L. Kreczko, S. Paramesvaran, L. Robertshaw, M.S. Sanjrani[39], J. Segal, V.J. Smith

Rutherford Appleton Laboratory, Didcot, United Kingdom
A.H. Ball, K.W. Bell, A. Belyaev[76], C. Brew, R.M. Brown, D.J.A. Cockerill, A. Elliot, K.V. Ellis, J. Gajownik, K. Harder, S. Harper, J. Linacre, K. Manolopoulos, M. Moallemi, D.M. Newbold, E. Olaiya, D. Petyt, T. Reis, A.R. Sahasransu, G. Salvi, T. Schuh, C.H. Shepherd-Themistocleous, I.R. Tomalin, K.C. Whalen, T. Williams

Imperial College, London, United Kingdom
I. Andreou, R. Bainbridge, P. Bloch, O. Buchmuller, C.A. Carrillo Montoya, D. Colling, I. Das, P. Dauncey, G. Davies, M. Della Negra, S. Fayer, G. Fedi, G. Hall, H.R. Hoorani, A. Howard, G. Iles, C.R. Knight, P. Krueper, J. Langford, K.H. Law, L. Lyons, A.-M. Magnan, B. Maier, S. Mallios, A. Mastronikolis, M. Mieskolainen, J. Nash[77], M. Pesaresi, P.B. Pradeep, B.C. Radburn-Smith, A. Richards, A. Rose, T.B. Runting, L. Russell, K. Savva, R. Schmitz, C. Seez, R. Shukla, A. Tapper, K. Uchida, G.P. Uttley, T. Virdee[27], N. Wardle, D. Winterbottom, J. Xiao

Brunel University, Uxbridge, United Kingdom
J.E. Cole, A. Khan, P. Kyberd, I.D. Reid

Baylor University, Waco, Texas, USA
S. Abdullin, A. Brinkerhoff, E. Collins, M.R. Darwish, J. Dittmann, K. Hatakeyama, V. Hegde, J. Hiltbrand, B. McMaster, J. Samudio, S. Sawant, C. Sutantawibul, J. Wilson

Bethel University, St. Paul, Minnesota, USA
J.M. Hogan

Catholic University of America, Washington, DC, USA
R. Bartek, A. Dominguez, S. Raj, B. Sahu, A.E. Simsek, B. Singhal, S.S. Yu

The University of Alabama, Tuscaloosa, Alabama, USA
B. Bam, A. Buchot Perraguin, S. Campbell, R. Chudasama, S.I. Cooper, C. Crovella, G. Fidalgo, S.V. Gleyzer, C. Isik, R. Kaur, A. Khukhunaishvili, K. Matchev, E. Pearson, P. Rumerio[78], E. Usai, R. Yi

Boston University, Boston, Massachusetts, USA
S. Cholak, G. De Castro, Z. Demiragli, C. Erice, C. Fangmeier, C. Fernandez Madrazo, J. Fulcher, J. Garcia De Castro, F. Golf, S. Jeon, J. O'Cain, I. Reed, J. Rohlf, K. Salyer, D. Sperka, I. Suarez, A. Tsatsos, E. Wurtz, A.G. Zecchinelli

Brown University, Providence, Rhode Island, USA
G. Barone, G. Benelli, D. Cutts, S. Ellis, L. Gouskos, M. Hadley, U. Heintz, K.W. Ho, T. Kwon, L. Lambrecht, G. Landsberg, K.T. Lau, M. LeBlanc, J. Luo, S. Mondal, J. Roloff, T. Russell, S. Sagir[79], X. Shen, M. Stamenkovic, S. Sunnarborg, J. Tang, N. Venkatasubramanian

University of California, Davis, Davis, California, USA
S. Abbott, S. Baradia, B. Barton, R. Breedon, H. Cai, M. Calderon De La Barca Sanchez, E. Cannaert, M. Chertok, M. Citron, J. Conway, P.T. Cox, F. Eble, R. Erbacher, C. Fairchild, O. Kukral, S. Ostrom, I. Salazar Segovia, J.H. Steenis, J.S. Tafoya Vargas, W. Wei, S. Yoo

University of California, Los Angeles, California, USA
K. Adamidis, H. Ancelin, M. Bachtis, D. Campos, R. Cousins, S. Crossley, G. Flores Avila, J. Hauser, M. Ignatenko, M.A. Iqbal, T. Lam, Y.f. Lo, E. Manca, A. Nunez Del Prado, D. Saltzberg, V. Valuev

University of California, Riverside, Riverside, California, USA
R. Clare, J.W. Gary, G. Hanson

University of California, San Diego, La Jolla, California, USA

A. Aportela, A. Arora, J.G. Branson, S. Cittolin, B. D'Anzi, D. Diaz, J. Duarte, L. Giannini, Y. Gu, J. Guiang, V. Krutelyov, R. Lee, J. Letts, H. Li, R. Marroquin Solares, M. Masciovecchio, F. Mokhtar, S. Mukherjee, M. Pieri, D. Primosch, M. Quinnan, V. Sharma, M. Tadel, E. Vourliotis, F. Würthwein, A. Yagil, Z. Zhao

University of California, Santa Barbara - Department of Physics, Santa Barbara, California, USA
A. Barzdukas, L. Brennan, C. Campagnari, S. Carron Montero[80], K. Downham, C. Grieco, M.M. Hussain, J. Incandela, M.W.K. Lai, A.J. Li, P. Masterson, J. Richman, S.N. Santpur, D. Stuart, T.Á. Vámi, X. Yan, D. Zhang

California Institute of Technology, Pasadena, California, USA
A. Albert, S. Bhattacharya, A. Bornheim, O. Cerri, Z. Hao, R. Kansal, L. Mori, H.B. Newman, G. Reales Gutiérrez, T. Sievert, P. Simmerling, M. Spiropulu, C. Sun, J.R. Vlimant, R.A. Wynne, S. Xie, R.Y. Zhu

Carnegie Mellon University, Pittsburgh, Pennsylvania, USA
J. Alison, S. An, M. Cremonesi, V. Dutta, E.Y. Ertorer, T. Ferguson, T.A. Gómez Espinosa, A. Harilal, A. Kallil Tharayil, M. Kanemura, A. Khanal, C. Liu, M. Marchegiani, P. Meiring, S. Murthy, P. Palit, K. Park, M. Paulini, A. Roberts, A. Sanchez, Y. Zhou

University of Colorado Boulder, Boulder, Colorado, USA
J.P. Cumalat, W.T. Ford, J. Fraticelli, A. Hart, M. Herrmann, S. Kwan, J. Pearkes, C. Savard, N. Schonbeck, K. Stenson, K.A. Ulmer, S.R. Wagner, N. Zipper, D. Zuolo

Cornell University, Ithaca, New York, USA
J. Alexander, X. Chen, J. Dickinson, A. Duquette, J. Fan, X. Fan, J. Grassi, P. Kotamnives, K. Krzyzanska, J. Monroy, G. Niendorf, M. Oshiro, J.R. Patterson, A. Ryd, J. Thom, H.A. Weber, B. Weiss, P. Wittich, Y. Wu, R. Zou, L. Zygala

Fermi National Accelerator Laboratory, Batavia, Illinois, USA
M. Albrow, M. Alyari, O. Amram, G. Apollinari, A. Apresyan, L.A.T. Bauerdick, D. Berry, J. Berryhill, P.C. Bhat, K. Burkett, J.N. Butler, A. Canepa, G.B. Cerati, H.W.K. Cheung, F. Chlebana, C. Cosby, G. Cummings, I. Dutta, V.D. Elvira, J. Freeman, A. Gandrakota, Z. Gecse, L. Gray, D. Green, A. Grummer, S. Grünendahl, D. Guerrero, O. Gutsche, R.M. Harris, J. Hirschauer, V. Innocente, B. Jayatilaka, S. Jindariani, M. Johnson, U. Joshi, R.S. Kim, B. Klima, S. Lammel, D. Lincoln, R. Lipton, T. Liu, K. Maeshima, D. Mason, P. McBride, P. Merkel, S. Mrenna, S. Nahn, J. Ngadiuba, D. Noonan, S. Norberg, V. Papadimitriou, N. Pastika, K. Pedro, C. Pena[81], C.E. Perez Lara, V. Perovic, F. Ravera, A. Reinsvold Hall[82], L. Ristori, M. Safdari, E. Sexton-Kennedy, E. Smith, N. Smith, A. Soha, L. Spiegel, S. Stoynev, J. Strait, L. Taylor, S. Tkaczyk, N.V. Tran, L. Uplegger, E.W. Vaandering, C. Wang, I. Zoi

University of Florida, Gainesville, Florida, USA
C. Aruta, P. Avery, D. Bourilkov, P. Chang, V. Cherepanov, M. Dittrich, R.D. Field, C. Huh, E. Koenig, M. Kolosova, J. Konigsberg, A. Korytov, G. Mitselmakher, K. Mohrman, A. Muthirakalayil Madhu, N. Rawal, S. Rosenzweig, V. Sulimov, Y. Takahashi, J. Wang

Florida State University, Tallahassee, Florida, USA
T. Adams, A. Al Kadhim, A. Askew, S. Bower, R. Goff, R. Hashmi, A. Hassani, T. Kolberg, G. Martinez, M. Mazza, H. Prosper, P.R. Prova, R. Yohay

Florida Institute of Technology, Melbourne, Florida, USA
B. Alsufyani, S. Das, S. Demarest, L. Hasa, M. Hohlmann, M. Lavinsky, E. Yanes

University of Illinois Chicago, Chicago, Illinois, USA
M.R. Adams, N. Barnett, A. Baty, C. Bennett, N. Brandman-hughes, R. Cavanaugh, R. Escobar Franco, O. Evdokimov, C.E. Gerber, H. Gupta, M. Hawksworth, A. Hingrajiya, D.J. Hofman, Z. Huang, J.h. Lee, C. Mills, S. Nanda, G. Nigmatkulov, B. Ozek, V. Pant, T. Phan, D. Pilipovic, R. Pradhan, E. Prifti, P. Roy, T. Roy, D. Shekar, N. Singh, F. Strug, A. Thielen, M.B. Tonjes, N. Varelas, M.A. Wadud, A. Wang, J. Yoo

The University of Iowa, Iowa City, Iowa, USA
M. Alhusseini, D. Blend, K. Dilsiz[83], O.K. Köseyan, A. Mestvirishvili[84], O. Neogi, H. Ogul[85], Y. Onel, A. Penzo, C. Snyder, E. Tiras[86]

Johns Hopkins University, Baltimore, Maryland, USA
B. Blumenfeld, J. Davis, A.V. Gritsan, Z. Huang, L. Kang, S. Kyriacou, P. Maksimovic, N. Pinto, M. Roguljic, S. Sekhar, M.V. Srivastav, M. Swartz

The University of Kansas, Lawrence, Kansas, USA
A. Abreu, L.F. Alcerro Alcerro, J. Anguiano, S. Arteaga Escatel, P. Baringer, A. Bean, R. Bhattacharya, Z. Flowers, D. Grove, J. King, G. Krintiras, M. Lazarovits, C. Le Mahieu, J. Marquez, M. Murray, M. Nickel, S. Popescu[87], C. Rogan, C. Royon, S. Rudrabhatla, S. Sanders, C. Smith, G. Wilson

Kansas State University, Manhattan, Kansas, USA
A. Ahmad, B. Allmond, N. Islam, A. Ivanov, K. Kaadze, Y. Maravin, J. Natoli, G.G. Reddy, D. Roy, G. Sorrentino

University of Maryland, College Park, Maryland, USA
A. Baden, A. Belloni, J. Bistany-riebman, S.C. Eno, N.J. Hadley, S. Jabeen, R.G. Kellogg, T. Koeth, B. Kronheim, S. Lascio, J. Lee, P. Major, A.C. Mignerey, C. Palmer, C. Papageorgakis, M.M. Paranjpe, E. Popova[88], A. Shevelev, L. Zhang

Massachusetts Institute of Technology, Cambridge, Massachusetts, USA
C. Baldenegro Barrera, H. Bossi, S. Bright-Thonney, I.A. Cali, Y.c. Chen, P.c. Chou, M. D'Alfonso, J. Eysermans, C. Freer, G. Gomez-Ceballos, M. Goncharov, G. Grosso, P. Harris, D. Hoang, G.M. Innocenti, K. Ivanov, G. Kopp, D. Kovalskyi, J. Lang, L. Lavezzo, Y.-J. Lee, P. Lugato, C. Mcginn, E. Moreno, A. Novak, M.I. Park, C. Paus, C. Reissel, C. Roland, G. Roland, S. Rothman, T.a. Sheng, G.S.F. Stephans, D. Walter, J. Wang, Z. Wang, B. Wyslouch, T. J. Yang

University of Minnesota, Minneapolis, Minnesota, USA
A. Alpana, B. Crossman, W.J. Jackson, C. Kapsiak, M. Krohn, D. Mahon, J. Mans, B. Marzocchi, R. Rusack, O. Sancar, R. Saradhy, N. Strobbe

University of Nebraska-Lincoln, Lincoln, Nebraska, USA
K. Bloom, D.R. Claes, S.V. Dixit, G. Haza, J. Hossain, C. Joo, I. Kravchenko, K.H.M. Kwok, Y. Mehra, J. Morris, A. Rohilla, J.E. Siado, A. Vagnerini, A. Wightman

State University of New York at Buffalo, Buffalo, New York, USA
H. Bandyopadhyay, L. Hay, H.w. Hsia, I. Iashvili, A. Kalogeropoulos, A. Kharchilava, A. Mandal, M. Morris, D. Nguyen, O. Poncet, S. Rappoccio, H. Rejeb Sfar, W. Terrill, A. Williams, D. Yu

Northeastern University, Boston, Massachusetts, USA
A. Aarif, G. Alverson, E. Barberis, S. Bein, J. Bonilla, B. Bylsma, M. Campana, R. Clark, J. Dervan, Y. Haddad, Y. Han, I. Israr, A. Krishna, M. Lu, N. Manganelli, R. Mccarthy, D.M. Morse, T. Orimoto, L. Skinnari, C.S. Thoreson, E. Tsai, D. Wood

Northwestern University, Evanston, Illinois, USA
S. Dittmer, K.A. Hahn, S. King, M. Mcginnis, Y. Miao, D.G. Monk, M.H. Schmitt, A. Taliercio, M. Velasco, J. Wang

University of Notre Dame, Notre Dame, Indiana, USA
G. Agarwal, R. Band, R. Bucci, S. Castells, A. Das, A. Datta, A. Ehnis, R. Goldouzian, M. Hildreth, K. Hurtado Anampa, T. Ivanov, C. Jessop, A. Karneyeu, K. Lannon, J. Lawrence, N. Loukas, L. Lutton, J. Mariano, N. Marinelli, P. Mastrapasqua, A. Masud, T. McCauley, C. Mcgrady, C. Moore, Y. Musienko[21], H. Nelson, M. Osherson, A. Piccinelli, R. Ruchti, A. Townsend, Y. Wan, M. Wayne, H. Yockey

The Ohio State University, Columbus, Ohio, USA
M. Carrigan, R. De Los Santos, L.S. Durkin, C. Hill, M. Joyce, D.A. Wenzl, B.L. Winer, B. R. Yates

Princeton University, Princeton, New Jersey, USA
H. Bouchamaoui, G. Dezoort, P. Elmer, A. Frankenthal, M. Galli, B. Greenberg, K. Kennedy, Y. Lai, D. Lange, A. Loeliger, D. Marlow, I. Ojalvo, J. Olsen, F. Simpson, D. Stickland, C. Tully, S. Yoon

University of Puerto Rico, Mayaguez, Puerto Rico, USA
S. Malik, R. Sharma

Purdue University, West Lafayette, Indiana, USA
S. Chandra, A. Gu, L. Gutay, M. Huwiler, M. Jones, A.W. Jung, I.G. Karslioglu, D. Kondratyev, J. Li, M. Liu, M. Macedo, G. Negro, N. Neumeister, G. Paspalaki, S. Piperov, N.R. Saha, J.F. Schulte, F. Wang, A.L. Wesolek, A. Wildridge, W. Xie, Y. Yao, Y. Zhong

Purdue University Northwest, Hammond, Indiana, USA
N. Parashar, A. Pathak, E. Shumka

Rice University, Houston, Texas, USA
D. Acosta, A. Agrawal, C. Arbour, T. Carnahan, K.M. Ecklund, F.J.M. Geurts, T. Huang, I. Krommydas, N. Lewis, W. Li, J. Lin, C. Loizides, O. Miguel Colin, B.P. Padley, R. Redjimi, J. Rotter, C. Vico Villalba, M. Wulansatiti, E. Yigitbasi, Y. Zhang

University of Rochester, Rochester, New York, USA
O. Bessidskaia Bylund, A. Bodek, P. de Barbaro[†], R. Demina, A. Garcia-Bellido, H.S. Hare, O. Hindrichs, N. Parmar, P. Parygin[88], H. Seo, R. Taus, Y.h. Yu

Rutgers, The State University of New Jersey, Piscataway, New Jersey, USA

B. Chiarito, J.P. Chou, S.V. Clark, S. Donnelly, D. Gadkari, Y. Gershtein, E. Halkiadakis, C. Houghton, D. Jaroslawski, A. Kobert, I. Laflotte, A. Lath, J. Martins, P. Meltzer, M. Perez Prada, B. Rand, J. Reichert, P. Saha, S. Salur, S. Somalwar, R. Stone, S.A. Thayil, S. Thomas, J. Vora

University of Tennessee, Knoxville, Tennessee, USA
A. Abdelhamid, D. Ally, A.G. Delannoy, S. Fiorendi, J. Harris, T. Holmes, A.R. Kanuganti, N. Karunarathna, J. Lawless, L. Lee, E. Nibigira, B. Skipworth, S. Spanier, A. Vendrasco

Texas A&M University, College Station, Texas, USA
D. Aebi, M. Ahmad, T. Akhter, K. Androsov, A. Basnet, A. Bolshov, O. Bouhali[89], A. Cagnotta, S. Cooperstein, V. D'Amante, R. Eusebi, P. Flanagan, J. Gilmore, Y. Guo, T. Kamon, S. Luo, R. Mueller, G. Pizzati, A. Safonov

Texas Tech University, Lubbock, Texas, USA
N. Akchurin, J. Damgov, Y. Feng, N. Gogate, W. Jin, S.W. Lee, C. Madrid, A. Mankel, T. Peltola, I. Volobouev

Vanderbilt University, Nashville, Tennessee, USA
E. Appelt, Y. Chen, S. Greene, A. Gurrola, W. Johns, R. Kunnawalkam Elayavalli, A. Melo, D. Rathjens, F. Romeo, P. Sheldon, S. Tuo, J. Velkovska, J. Viinikainen, J. Zhang

University of Virginia, Charlottesville, Virginia, USA
B. Cardwell, H. Chung, B. Cox, J. Hakala, G. Hamilton Ilha Machado, R. Hirosky, M. Jose, A. Ledovskoy, C. Mantilla, C. Neu, C. Ramón Álvarez, Z. Wu

Wayne State University, Detroit, Michigan, USA
S. Bhattacharya, P.E. Karchin

University of Wisconsin - Madison, Madison, Wisconsin, USA
A. Aravind, S. Banerjee, K. Black, T. Bose, E. Chavez, R. Cruz, S. Dasu, P. Everaerts, C. Galloni, H. He, M. Herndon, A. Herve, C.K. Koraka, S. Lomte, R. Loveless, A. Mallampalli, J. Marquez, A. Mohammadi, S. Mondal, T. Nelson, G. Parida, L. Pétré, D. Pinna, A. Savin, V. Shang, V. Sharma, R. Simeon, W.H. Smith, D. Teague, M. Thakore, A. Thete, A. Warden

Authors affiliated with an international laboratory covered by a cooperation agreement with CERN
S. Afanasiev, V. Alexakhin, Yu. Andreev, T. Aushev, D. Budkouski, R. Chistov, M. Danilov, T. Dimova, A. Ershov, S. Gninenko, I. Gorbunov, A. Kamenev, V. Karjavine, M. Kirsanov, V. Klyukhin, O. Kodolova[90], V. Korenkov, I. Korsakov, A. Kozyrev, N. Krasnikov, A. Lanev, A. Malakhov, V. Matveev, A. Nikitenko[91,90], V. Palichik, V. Perelygin, O. Radchenko, M. Savina, V. Shalaev, S. Shmatov, S. Shulha, Y. Skovpen, K. Slizhevskiy, V. Smirnov, O. Teryaev, I. Tlisova, A. Toropin, N. Voytishin, A. Zarubin, I. Zhizhin

Authors affiliated with an institute formerly covered by a cooperation agreement with CERN
L. Dudko, V. Kim[21], V. Murzin, V. Oreshkin, D. Sosnov

†: Deceased
[1]Also at Yerevan State University, Yerevan, Armenia
[2]Also at TU Wien, Vienna, Austria

[3]Also at Ghent University, Ghent, Belgium
[4]Also at FACAMP - Faculdades de Campinas, Sao Paulo, Brazil
[5]Also at Universidade Estadual de Campinas, Campinas, Brazil
[6]Also at Federal University of Rio Grande do Sul, Porto Alegre, Brazil
[7]Also at The University of the State of Amazonas, Manaus, Brazil
[8]Also at University of Chinese Academy of Sciences, Beijing, China
[9]Also at University of Chinese Academy of Sciences, Beijing, China
[10]Also at School of Physics, Zhengzhou University, Zhengzhou, China
[11]Now at Henan Normal University, Xinxiang, China
[12]Also at University of Shanghai for Science and Technology, Shanghai, China
[13]Also at The University of Iowa, Iowa City, Iowa, USA
[14]Also at Nanjing Normal University, Nanjing, China
[15]Also at Center for High Energy Physics, Peking University, Beijing, China
[16]Also at Cairo University, Cairo, Egypt
[17]Also at Suez University, Suez, Egypt
[18]Now at British University in Egypt, Cairo, Egypt
[19]Also at Université de Haute Alsace, Mulhouse, France
[20]Also at Purdue University, West Lafayette, Indiana, USA
[21]Also at an institute formerly covered by a cooperation agreement with CERN
[22]Also at University of Hamburg, Hamburg, Germany
[23]Also at RWTH Aachen University, III. Physikalisches Institut A, Aachen, Germany
[24]Also at Bergische University Wuppertal (BUW), Wuppertal, Germany
[25]Also at Brandenburg University of Technology, Cottbus, Germany
[26]Also at Forschungszentrum Jülich, Juelich, Germany
[27]Also at CERN, European Organization for Nuclear Research, Geneva, Switzerland
[28]Also at HUN-REN ATOMKI - Institute of Nuclear Research, Debrecen, Hungary
[29]Now at Universitatea Babes-Bolyai - Facultatea de Fizica, Cluj-Napoca, Romania
[30]Also at MTA-ELTE Lendület CMS Particle and Nuclear Physics Group, Eötvös Loránd University, Budapest, Hungary
[31]Also at HUN-REN Wigner Research Centre for Physics, Budapest, Hungary
[32]Also at Physics Department, Faculty of Science, Assiut University, Assiut, Egypt
[33]Also at The University of Kansas, Lawrence, Kansas, USA
[34]Also at Punjab Agricultural University, Ludhiana, India
[35]Also at University of Hyderabad, Hyderabad, India
[36]Also at Indian Institute of Science (IISc), Bangalore, India
[37]Also at University of Visva-Bharati, Santiniketan, India
[38]Also at Institute of Physics, Bhubaneswar, India
[39]Also at Deutsches Elektronen-Synchrotron, Hamburg, Germany
[40]Also at Isfahan University of Technology, Isfahan, Iran
[41]Also at Sharif University of Technology, Tehran, Iran
[42]Also at Department of Physics, University of Science and Technology of Mazandaran, Behshahr, Iran
[43]Also at Department of Physics, Faculty of Science, Arak University, ARAK, Iran
[44]Also at Helwan University, Cairo, Egypt
[45]Also at Italian National Agency for New Technologies, Energy and Sustainable Economic Development, Bologna, Italy
[46]Also at Centro Siciliano di Fisica Nucleare e di Struttura Della Materia, Catania, Italy
[47]Also at James Madison University, Harrisonburg, Maryland, USA
[48]Also at Università degli Studi Guglielmo Marconi, Roma, Italy

[49]Also at Scuola Superiore Meridionale, Università di Napoli 'Federico II', Napoli, Italy
[50]Also at Fermi National Accelerator Laboratory, Batavia, Illinois, USA
[51]Also at Lulea University of Technology, Lulea, Sweden
[52]Also at Consiglio Nazionale delle Ricerche - Istituto Officina dei Materiali, Perugia, Italy
[53]Also at UPES - University of Petroleum and Energy Studies, Dehradun, India
[54]Also at Institut de Physique des 2 Infinis de Lyon (IP2I), Villeurbanne, France
[55]Also at Department of Applied Physics, Faculty of Science and Technology, Universiti Kebangsaan Malaysia, Bangi, Malaysia
[56]Also at Trincomalee Campus, Eastern University, Sri Lanka, Nilaveli, Sri Lanka
[57]Also at Saegis Campus, Nugegoda, Sri Lanka
[58]Also at National and Kapodistrian University of Athens, Athens, Greece
[59]Also at Ecole Polytechnique Fédérale Lausanne, Lausanne, Switzerland
[60]Also at Universität Zürich, Zurich, Switzerland
[61]Also at Stefan Meyer Institute for Subatomic Physics, Vienna, Austria
[62]Also at Near East University, Research Center of Experimental Health Science, Mersin, Turkey
[63]Also at Konya Technical University, Konya, Turkey
[64]Also at Istanbul Topkapi University, Istanbul, Turkey
[65]Also at Izmir Bakircay University, Izmir, Turkey
[66]Also at Adiyaman University, Adiyaman, Turkey
[67]Also at Bozok Universitetesi Rektörlügü, Yozgat, Turkey
[68]Also at Istanbul Sabahattin Zaim University, Istanbul, Turkey
[69]Also at Marmara University, Istanbul, Turkey
[70]Also at Milli Savunma University, Istanbul, Turkey
[71]Also at Informatics and Information Security Research Center, Gebze/Kocaeli, Turkey
[72]Also at Kafkas University, Kars, Turkey
[73]Now at Istanbul Okan University, Istanbul, Turkey
[74]Also at Istanbul University - Cerrahpasa, Faculty of Engineering, Istanbul, Turkey
[75]Also at Istinye University, Istanbul, Turkey
[76]Also at School of Physics and Astronomy, University of Southampton, Southampton, United Kingdom
[77]Also at Monash University, Faculty of Science, Clayton, Australia
[78]Also at Università di Torino, Torino, Italy
[79]Also at Karamanoğlu Mehmetbey University, Karaman, Turkey
[80]Also at California Lutheran University, Thousand Oaks, California, USA
[81]Also at California Institute of Technology, Pasadena, California, USA
[82]Also at United States Naval Academy, Annapolis, Maryland, USA
[83]Also at Bingol University, Bingol, Turkey
[84]Also at Georgian Technical University, Tbilisi, Georgia
[85]Also at Sinop University, Sinop, Turkey
[86]Also at Erciyes University, Kayseri, Turkey
[87]Also at Horia Hulubei National Institute of Physics and Nuclear Engineering (IFIN-HH), Bucharest, Romania
[88]Now at another institute formerly covered by a cooperation agreement with CERN
[89]Also at Hamad Bin Khalifa University (HBKU), Doha, Qatar
[90]Also at Yerevan Physics Institute, Yerevan, Armenia
[91]Also at Imperial College, London, United Kingdom